nature ecology & evolution

ARTICLES

https://doi.org/10.1038/s41559-018-0781-2

Epigenetic gene silencing alters the mechanisms and rate of evolutionary adaptation

Dragan Stajic[1], Lília Perfeito[1*] and Lars E. T. Jansen[1,2*]

Epigenetic, non-DNA sequence-based inheritance can potentially contribute to adaptation but, due to its transient nature and the difficulty involved in uncoupling it from genetic variation, it is unclear whether it has any effect on long-term evolution. However, short-term epigenetic inheritance may interact with genetic change by modifying the rate and type of adaptive mutations. Here, we test this notion in an experimental evolution set-up in yeast. We tune low, intermediate and high levels of heritable silencing of a *URA3* reporter under selection by insertion at different positions within silent subtelomeric chromatin in otherwise isogenic *Saccharomyces cerevisiae*. Heritable silencing does not impact mutation rate but drives population size expansion and rapid epigenetic adaptation. This eventually leads to genetic assimilation of the silent phenotype by mutations that reduce or abolish *URA3* expression. Moreover, at intermediate or low levels of heritable silencing we find that populations evolve more rapidly by accumulation of adaptive mutations, in part through acquisition of novel alleles that enhance gene silencing, aiding accelerated adaptation. We provide an experimental proof of concept that defines the impact and mechanisms of how short-term epigenetic inheritance can shape adaptive evolution.

Natural selection acts on heritable variation in fitness-related traits. Gene expression states that confer phenotypes can be inherited epigenetically and could therefore, in principle, contribute to adaptive evolution. While such epigenetic inheritance is relatively short-lived, it can persist for a number of generations and contribute to selectable phenotypic variation, as highlighted for example by work on plants and worms[1–3]. Unlike genetic mutations, epi-mutations occur frequently and are generally transient and reversible, a property fundamentally different from mutations in DNA where reversion of a change is typically rare. Transient forms of phenotypic inheritance may facilitate adaptation under conditions of a novel stressful environment where evolutionary rescue by mutation may be difficult. In such a scenario, temporary epigenetic change may provide phenotypic variation, allowing adaptation before the appearance of mutations. This is a form of genetic assimilation akin to either the Baldwin effect[4] or canalization proposed by Waddington[5,6] and, more recently, demonstrated in the context, for example, of HSP90-mediated evolution[7,8] or in the case of prion-mediated epigenetic states[9]. In the latter case, stable conformers of proteins are cytoplasmically inherited and impact on cellular fitness[10]. While these are unique specialized cases of epigenetic inheritance, gene expression states can also be epigenetically maintained, including trans-generationally in a variety of organisms, particularly in plants[3] and *Caenorhabditis elegans*[11], but also in more complex metazoans, including flies and mammals[12]. As gene expression is fundamental to phenotypic variation, this form of heritability of chromatin states has the potential to be of broad relevance to the dynamics of adaptation.

For this reason we now ask: to what extent and with what consequences can chromatin-based, epigenetically heritable gene silencing contribute to adaptation? Recent theory predicts that an epigenetic form of inheritance can be an effective means of reaching a fitness optimum quickly by acting as a buffering step until mutations fix in the population. This can be achieved by facilitating the survival of the population in a new environment, giving it time to accumulate adaptive mutations[13,14]. Models suggest there might be an optimal degree of the stability of epigenetic inheritance that can speed up evolution[15]. Despite the growing body of theoretical efforts, direct experimental evidence is still lacking as pointed out recently[16], and one can envisage different scenarios where epigenetic forms of inheritance can either impede or aid adaptation. Here we directly test these theoretical predictions with a powerful experimental evolution set-up that allows us to distinguish the contribution to adaptation of genetic mutations versus transiently heritable changes in gene expression. The strength of this system is dependent on the ability to control the clonality (that is, no standing genetic variation) of the population and the rate of epigenetic modification. Key questions that we address are: how does short-lived but heritable gene silencing impact (1) the rate of fitness increase, (2) the spread of new beneficial mutations and, ultimately, (3) the adaptation of a population?

Results

In the budding yeast, *Saccharomyces cerevisiae*, genes proximal to mating type loci, ribosomal DNA arrays and telomeres undergo heritable gene silencing, dependent on the silent information regulator (SIR) proteins[17–19] that act, in part, via deacetylation of local chromatin[20]. This classic epigenetic mechanism is initiated by sequence-specific DNA binding proteins that nucleate a local self-perpetuating feedback system where hypo-acetylated nucleosomes form an anchor for recruitment of additional SIR complexes allowing for local spreading of silencing[21]. Consequently, genes located at, or adjacent to, these loci are silenced in a SIR-dependent manner[22]. Importantly, while sequence elements are required to target silencing, the silencing itself is subject to stochastic switching between ON and OFF states, both of which are heritable for multiple divisions. Therefore, silencing in this context relates to the switching rate of gene silencing versus activation, leading to an equilibrium between two interchanging subpopulations[23]. The rate of switching is dependent on position and local chromatin context[22].

[1]Instituto Gulbenkian de Ciência, Oeiras, Portugal. [2]Department of Biochemistry, University of Oxford, Oxford, UK. *e-mail: lperfeito@igc.gulbenkian.pt; lars.jansen@bioch.ox.ac.uk

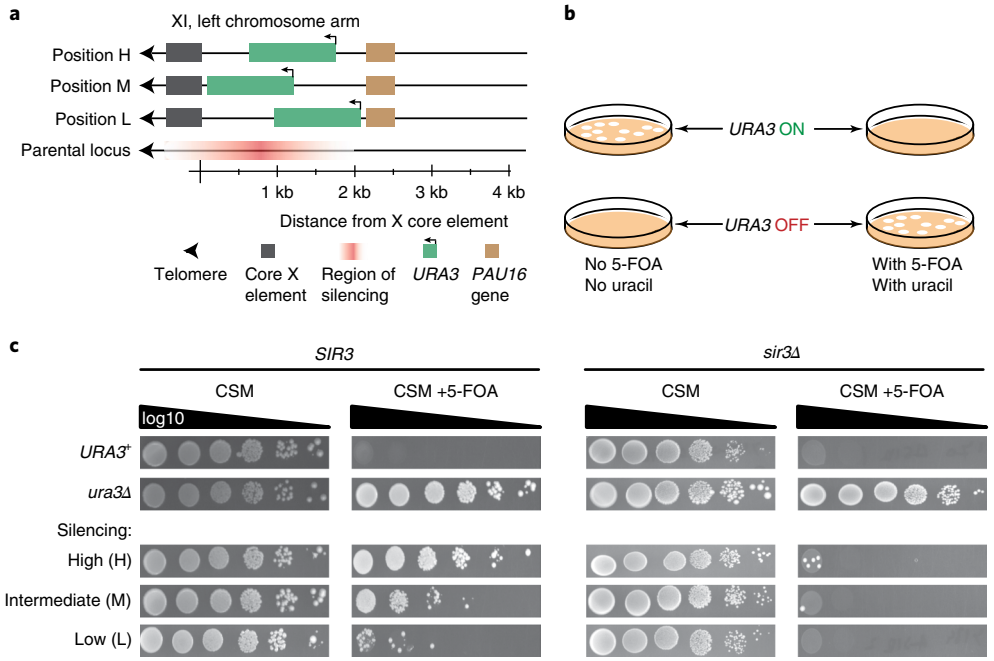

Fig. 1 | Outline and characterization of experimental system. a, Scheme showing positions of *URA3* gene cassette in different yeast strains relative to the core X element near the telomere on the left arm of chromosome XI. **b**, Scheme outlining the principle of counter-selection using *URA3* as reporter gene. Ura3 is essential for biosynthesis of uracil (positive selection in the absence of uracil), but converts the drug 5-FOA into a toxin that kills the cell (negative selection). **c**, Measurement of the relative strength of silencing. Tenfold dilutions of indicated strains were spotted on either plates containing 5-FOA or minimal, non-selective media plates as control for growth. The strains *ura3Δ* and *URA3+* were used as positive and negative controls, respectively. Deletion of *SIR3* resulted in loss of silencing at all *URA3* insertion positions[17].

An experimental evolution set-up based on tuneable SIR-mediated heritable gene silencing. We constructed an allelic series of *S. cerevisiae* strains in which we inserted a functional *URA3* cassette at seven different positions ordered along the subtelomeric region of the left arm of chromosome XI (Supplementary Fig. 1a), thereby tuning the degree of epigenetic switching in otherwise isogenic clones. This puts us in a unique position to quantitatively assess the contribution of epigenetic silencing to adaptation. *URA3* is a widely used reporter gene that can be subjected to both positive and negative selection. Functional Ura3 protein is essential for uracil biosynthesis and is required for growth in the absence of uracil, but induces cell death in the presence of the drug 5-fluoroorotic acid (5-FOA, Fig. 1b)[24]. Consequently, *URA3* gene silencing leads to resistance to 5-FOA, a phenotypic trait previously used to study the nature of heritable epigenetic silencing in yeast, estimated to be maintained for up to 20 generations[25]. We assayed the degree of silencing of *URA3* at different subtelomeric positions by real-time growth rate measurements under different concentrations of 5-FOA, titrating the selective pressure within our experimental evolution set-up (Supplementary Fig. 1b). As expected from previous reports[22], we found that the degree of silencing in our allelic series roughly scales with the distance from the telomere but is discontinuous as reported[26], with the strongest silencing observed at about 2 kilobases (kb) from the telomere (Supplementary Fig. 1b, position 5) and declining in either direction, where positions 6 and 7 (closer to the telomere end) displayed intermediate levels of silencing and positions 4, 3, 2 and 1 (distal to the SIR seeding point) represented low silencing levels (Supplementary Fig. 1).

From our allelic series, we selected three *URA3* insertion loci representing low (L), intermediate (M) and high (H) silencing, henceforth simply named L, M and H, respectively, denoting the degree of silencing (Supplementary Fig. 1 and 1a). Spot growth assays on 5-FOA confirmed the different degrees of silencing (Fig. 1c). These strains, which are otherwise isogenic, formed the basis of our experimental evolution strategy where we can vary the level of epigenetic gene silencing (dictated by the *URA3* position) as well as the selective pressure (5-FOA concentration). As expected[18], silencing at all positions was SIR complex dependent (Fig. 1c, right panel).

Intermediate levels of heritable gene silencing accelerate adaptation. Our experimental set-up allowed us to determine the dynamics and mechanisms of adaptation in a highly defined system where a single pathway is under selection in the presence or absence of short-term heritable gene silencing. Cells were first pre-selected, in complete synthetic media (CSM) lacking uracil, to ensure that all strains were in the *URA*$^+$ state at the onset of the experiment, irrespective of their ability to silence. Each population was then evolved by serial daily passage into liquid culture containing 0.05% 5-FOA (Fig. 2a), a dose conferring intermediate selection pressure in which all strains proliferate in a manner dependent on the degree of *URA3* silencing (Supplementary Fig. 1b). Half a million cells were transferred daily under continued selection, and the number of living cells in each of the 24 replicates per strain was determined by plating on non-selective media. In parallel, cells were plated on high concentrations of 5-FOA to determine the fraction adapted to growth under selection. Furthermore, these 5-FOA-resistant clones were replica-plated on medium lacking uracil to determine whether adaptation would occur while maintaining the ability to switch on *URA3* expression (where growth indicates the ability to reactivate *URA3*) or by directly affecting the uracil biosynthetic pathway (for example, by mutation of *URA3*), in which case cells can no longer grow in the absence of uracil. As expected, the strain with higher levels of epigenetic silencing survived better on encountering 5-FOA (Fig. 2b, H–M: $P < 0.0001$ at 48 h; H–L: $P < 0.0001$ at 48 h ($N = 24$ for H and M, 21 for L), Tukey honestly significant difference). These populations adapted very rapidly, reaching maximum resistance rates after 24–48 h (Fig. 2c and Supplementary Fig. 2).

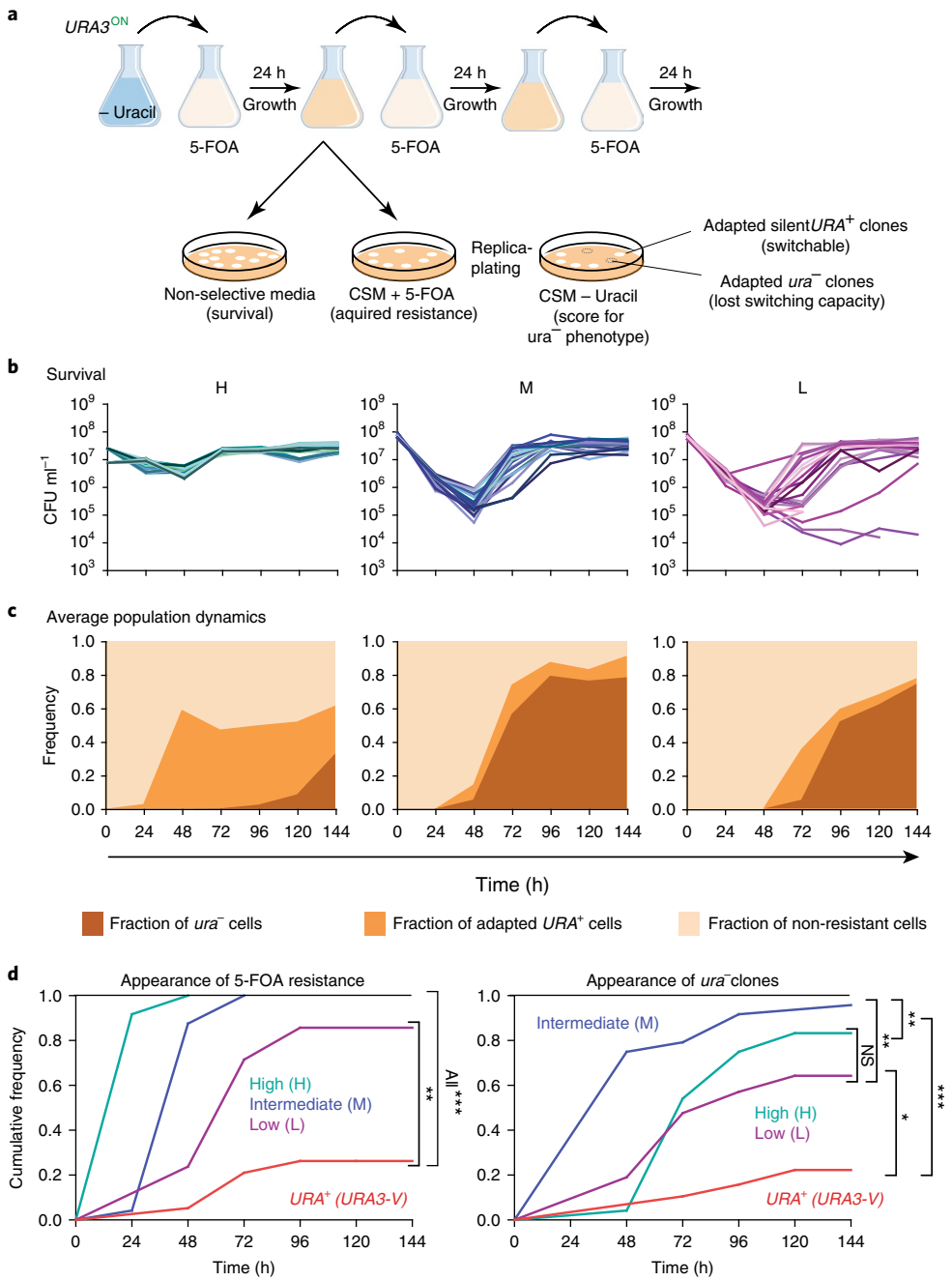

Fig. 2 | Intermediate epigenetic gene silencing enables better survival and faster adaptation in a new environment. a, Experimental set-up. Populations were pre-selected in media lacking uracil (all cells expressing *URA3*) and evolved in liquid CSM with 0.05% 5-FOA. Every 24 h cells were passed for further selection and scored for both viability (based on the number of colonies on non-selective plates) and acquisition of 5-FOA resistance (number of colonies growing on 5-FOA selection). 5-FOA-resistant clones were replica-plated onto CSM plates without uracil (growth indicates that cells are *ura*$^+$, despite being 5-FOA resistant, for example, due to epigenetic silencing); lack of growth indicates that cells are *ura*$^-$. **b**, Survival through the course of selection (as determined by the number of colony-forming units - CFU - per millilitre. Each line represents the number of living cells in each replicate population—24 parallel populations for *URA3* positions H and M and 21 for L (strains LJY186, LJY188 and LJY185, respectively, see Supplementary Fig. 9). **c**, Dynamics of the acquisition of 5-FOA resistance. Coloured areas represent the different phenotypic subgroups within each population (as indicated), plotted as the size fraction of each subgroup within the total population across time. The graphs represent the median value of all replicate populations (see Supplementary Fig. 2 for complete dataset). **d**, Cumulative frequency of populations that acquired at least one detectable resistant clone (left), or resistant with a *ura*$^-$ phenotype (right) during the course of the experiment. Evolution of a strain with *URA3* at its endogenous position on chromosome V (*URA*-V, which is not subject to silencing) is included as control (see Supplementary Fig. 3 for complete *URA*-V dataset). Differences between strains were compared using the log-rank test with Bonferroni correction for multiple testing (N_H and $N_M = 24$, $N_L = 21$, $N_{WT} = 19$). Appearance of resistance: $P_{M\text{-}URA3\text{-}V}$, $P_{M\text{-}H}$, $P_{M\text{-}L}$, $P_{H\text{-}URA3\text{-}V}$ and $P_{H\text{-}L}$ all 10^{-4} (***), $P_{L\text{-}URA3\text{-}V} < 2\times10^{-4}$ (**). Appearance of mutations: $P_{M\text{-}URA3\text{-}V} < 10^{-4}$ (***), $P_{M\text{-}H} < 1.6\times10^{-3}$ (**), $P_{M\text{-}L} < 1.1\times10^{-3}$(**), $P_{H\text{-}URA3\text{-}V} < 10^{-4}$(***), $P_{L\text{-}URA3\text{-}V} < 5\times10^{-3}$ (*), $P_{H\text{-}L} < 0.396$; NS, not significant.

Importantly, the frequency of resistance in the *URA3*-H populations, after the initial rapid increase, reached an equilibrium at approximately 50% (Fig. 2c) that was maintained throughout the length of the experiment (~90 generations), presumably reflecting the frequent switching of the silent *URA3*^{OFF} state to an *URA3*^{ON} state. Genetically *ura*$^-$ clones appeared late (median time of initial detection, 72 h) and took longer to spread among the population. Such dynamics probably resulted from competition between clones carrying de novo mutations and heritably silenced clones, delaying the increase in frequency of mutants, a phenomenon analogous to clonal interference[27]. Contrary to the strong capacity of the high-silencing strain (H) to withstand a novel stressful environment due to heritably low expression of *URA3*, in the strain with low levels of silencing (L), population sizes dropped by more than two orders of magnitude (Fig. 2b) due to a high degree of deleterious *URA3* expression and inability to adapt epigenetically. These strains therefore adapted more slowly (Fig. 2c). In addition, extinction was detected in 4/21 replicates (Fig. 2b and Supplementary Fig. 2, *URA3*-L), demonstrating the power of epigenetic silencing in rescuing populations.

Interestingly, at intermediate levels of silencing (*URA3*-M) cells adapted more rapidly, initially while maintaining the capacity to switch followed by the appearance of *ura*$^-$ clones (median time of initial detection, 48 h). To quantify these differences, we calculated (1) the frequency of acquisition of adaptive 5-FOA resistance (typically through silencing) and (2) the frequency of appearance of adaptive *ura*$^-$ clones, which most probably reflects genetic mutations across all evolved populations (Fig. 2d). This analysis shows that the rate of initial resistance scales with the degree of silencing, while the appearance and spread of adaptive *ura*$^-$ clones is accelerated at the intermediate level of silencing (Fig. 2d). In 18 out of 24 (*URA3*-M) populations, over 50% of clones were fully *ura*$^-$ compared to only eight populations under high silencing (*URA3*-H) ($P=0.008$, $N=24$, Fisher's exact test). This indicates an optimal degree of short-term heritable gene silencing that impacts long-term adaptation.

In contrast, these differences in adaptation dynamics disappeared in cells in which *URA3* could not be silenced. In WT SIR$^+$-competent cells in which *URA3* is at its endogenous centromere-proximal location on chromosome V (*URA3*-V, no silencing), we found that the majority of evolved populations went extinct (14 out of 19 populations) with adaptive mutations arising infrequently (Supplementary Fig. 3 and Fig. 2d (red line)). This shows that the lack of silencing dramatically hinders the ability to adapt under these experimental conditions. In strains bearing subtelomeric *URA3* but lacking silencing (by deletion of *SIR3*), we found that *ura3*$^-$ mutants appeared more frequently compared to WT cells (Supplementary Fig. 4). This was probably due to an overall increase in mutation rate by recombination (Supplementary Fig. 5, see below) at defective telomeres[28]. Importantly, in the absence of silencing, all three *URA3* insertion positions behaved virtually identically, with a median time of appearance for *ura*$^-$ clones of 72 h (eight replicate populations each; Supplementary Fig. 4b), which is still slower compared to strains with moderate *URA3* silencing (Fig. 2c). These experiments further underscore the notion that the differences between the degrees of adaptability of strains L, M and H are due to silencing rather than to intrinsic sequence differences between *URA3* positions.

Adaptation dynamics cannot be explained by local differences in mutation rate. To determine whether the differences in adaptation rates could be explained by intrinsic differences in mutation frequencies among the different *URA3* insertion sites, we performed Luria–Delbrück fluctuation assays[29] in either the presence (*SIR3*) or absence of silencing (*sir3Δ*) (Supplementary Fig. 5). In strains devoid of subtelomeric silencing, overall mutation frequencies were increased by around twofold, probably due to increased recombination in the absence of subtelomeric silencing and consequent loss of telomeric chromatin organization, as reported[22,28]. However, no differences were found among the *URA3* sites, indicating that the position of the reporter has no bearing on mutation rates. Similarly, when mutations were allowed to accumulate in the presence of normal subtelomeric silencing, mutation rates were similar across *URA3* positions. It should be noted that, even in the presence of silencing, subtelomeric regions generally have higher mutation rates due to elevated rates of recombination relative to telomere distal sites[30,31]. Indeed, PCR analysis of evolved clones revealed that the *URA3* gene was lost in the majority of *ura*$^-$ clones (16/16 of *URA3*-M clones, 11/13 *URA3*-H clones and 10/14 *URA3*-L clones). While we do not have the statistical power to evaluate the significance of these differences ($P_{M-H}=0.1921$, $P_{M-L}=0.0365$, $P_{H-L}=0.6483$, Fisher's exact test), high recombination rates were similar across the different subtelomeric insertion positions and have no bearing on the overall mutation frequency (Supplementary Fig. 5). These results indicate that epigenetically heritable gene silencing has a dominant role in explaining the differences in adaptation, rather than genetic differences in mutation frequencies due to local sequence or chromatin effects. Combined, these data suggest that heritable gene silencing results in faster acquisition of typical *ura*$^-$ mutations. This is indicative of a form of genetic assimilation where short-term epigenetic silencing precedes adaptation by mutation.

Heritable gene silencing expands the mutation target for adaptation. To uncover the genetic basis of adaptation, we performed whole-genome sequencing on 10–12 independently evolved clones per position, from both the *ura*$^-$ class and resistant but switchable *URA*$^+$ clones. Sequencing revealed that most *ura*$^-$ clones had resulted from a subtelomeric deletion containing the *URA3* cassette (as predicted from our PCR analysis above), probably due to a high rate of gene conversion at subtelomeric regions (Supplementary Fig. 6), consistent with the high mutation rate estimation in the fluctuation test (Supplementary Fig. 5). Interestingly, in six out of six evolved *URA3*-H and two out of six evolved *URA3*-M and *URA3*-L clones, we were unable to identify any causative mutation. While the idea that these adapted purely epigenetically is tantalizing, we cannot exclude the possibility that these clones either bear an undetected mutation or represent the ancestral lineages that survived until the end of the experiment.

Importantly, we observed an expansion of the mutational target beyond the *URA3* gene in clones from populations with low or intermediate levels of silencing showing rapid adaptation (Supplementary Fig. 6, *URA3*-M and *URA3*-L). In these strains we found, in addition to *URA3* mutations in *ura*$^-$ clones, unlinked mutations in adapted *URA*$^+$ clones. Of specific interest are novel mutations in *PPR1*, a known trans-activator of *URA3* that has previously been shown to collaborate with SIR-mediated silencing. *PPR1* mutants enhance telomere repression of *URA3* at more distal positions from the telomere in a SIR-dependent manner[32,33]. This exemplifies how heritable gene silencing can render specific mutational targets such as *PPR1* relevant for adaptation. We found this form of adaptation in three independent clones in populations with low and intermediate silencing. Furthermore, we recovered a non-synonymous mutation in the *RPD3* gene, a histone deacetylase with known roles in gene silencing, where it has been shown to directly oppose SIR-mediated silencing[34].

Novel alleles enhance heritable gene silencing, resulting in increased fitness. To determine whether the evolved populations that acquired mutations outside of *URA3* had produced adapted clones, we estimated fitness by measuring the direct growth rates of clones in 0.05% 5-FOA (Fig. 3). Most evolved clones derived from medium- and low-silencing ancestors (*URA3*-M and *URA3*-L,

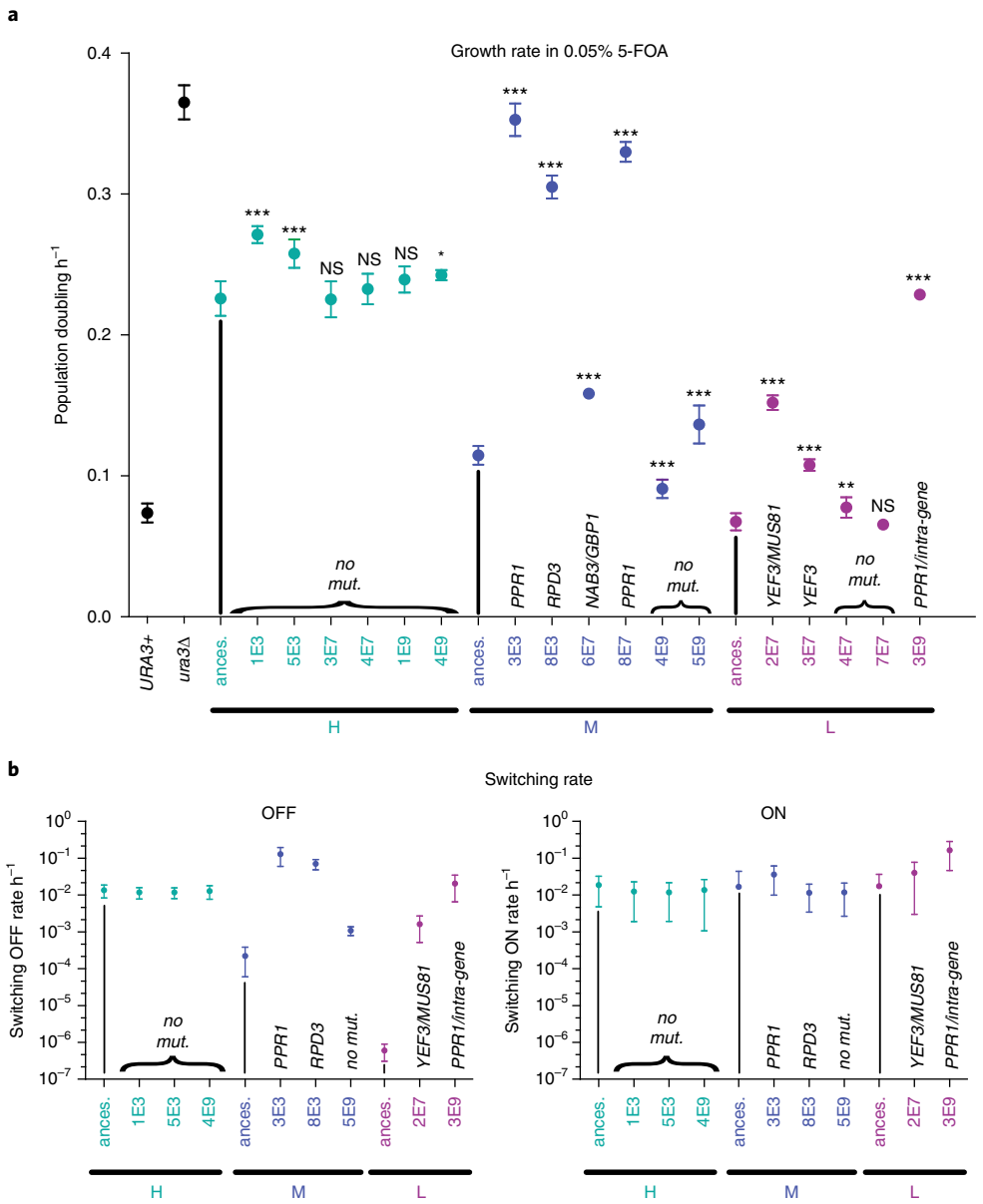

Fig. 3 | Evolved clones increase fitness by changing the epigenetic switching rate of URA3 gene silencing. a, Growth rate of control strains. Ancestral and evolved *URA*$^+$ clones were determined in liquid culture under selection in 0.05% 5-FOA. Mean and one standard deviation of nine replicate populations are shown. Indicated *P* values are pairwise *t*-test comparisons between evolved clones and the ancestral strain, with Bonferroni correction for multiple testing. Calculated *P* values ($N=9$): M clones: 3E3 , $<2\times10^{-16}$; 8E3, $<2\times10^{-16}$; 6E7, 1.9×10^{-13}; 8E7, $<2\times10^{-16}$; 4E9, 2.1×10^{-5}; 5E9, 2.1×10^{-5}. H clones: 1E3, $<1.3\times10^{-12}$; 5E3, $<8.6\times10^{-8}$; 3E7, 1.0 NS; 4E7, 1.0 NS; 1E9, 0.0892 NS; 4E9, 0.0127 NS. L clones: 2E7, $<2\times10^{-16}$; 3E7, $<2\times10^{-16}$; 4E7, 0.0015; 7E7, 1.0 NS; 3E9, $<2\times10^{-16}$. NS, not significant. **b**, Estimated switching rates. Based on the *URA3*^{ON} to *URA3*^{OFF} curves presented in Supplementary Fig. 8, we estimated the probability that cells either switch off *URA3* (left plot) or switch on *URA3* (right plot) (see Methods). Fitting of data from four experiments with 95% confidence intervals is shown. For each *URA3* position the growth rate of the ancestral (ances.) clones is highlighted with a vertical bar, and evolved clones are plotted in the corresponding colour. *URA3*-H clones are green, *URA3*-M clones are blue and *URA3*-L clones are magenta. The identified mutations in Supplementary Fig. 6 are included in the graph for clarity.

respectively) showed an increase in fitness in 5-FOA. In particular, those with mapped mutations in *PPR1* and *RPD3* showed strong adaptation (~2.5- to 3.5-fold increase in growth rate), approaching the growth rate of a *ura3Δ* strain, despite maintaining an intact *URA3* locus. Several clones in which no mutation could be identified also showed a significant increase in fitness, although in this case the effect was much more modest (~1.05- to 1.2-fold increase in growth rate, Fig. 3). Due to these small changes in growth rates, we cannot exclude the possibility that these clones are ancestral lineages that survived selection.

The identification of mutations outside of *URA3*, particularly those with known roles in gene silencing such as *PPR1* and *RPD3*, prompted us to determine whether *URA+* evolved mutant clones adapted by modulating epigenetic silencing or through independent means. We exposed these clones to nicotinamide, a known inhibitor of SIR2 activity that reduces silencing[35]. Strikingly, SIR2 inhibition abolished 5-FOA resistance in all evolved clones that had maintained epigenetic switching (Supplementary Fig. 7), indicating that the acquired resistance to 5-FOA is increased in a SIR-dependent manner. This demonstrates a mechanism of adaptation

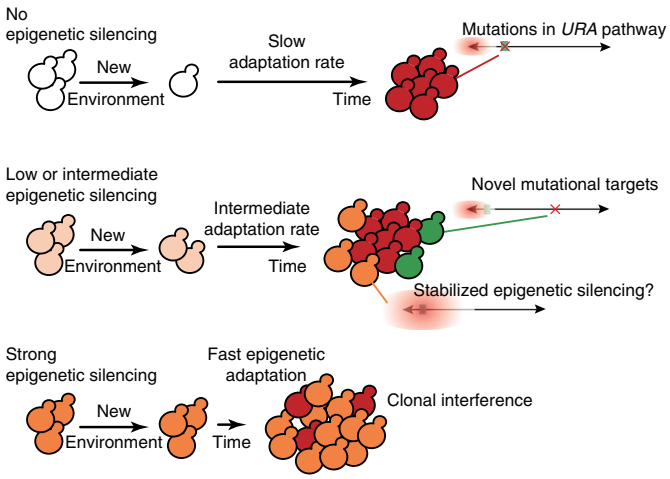

Fig. 4 | Observed and potential pathways to adaptation and the contribution of epigenetic silencing. Populations with no epigenetic silencing adapt through acquisition of mutations, mostly in the *URA3* gene locus[29] at a low frequency (red cells). Intermediate levels of heritable gene silencing allow the expansion of population size (yellow cells) and result in the appearance of novel mutational targets (green cells) that may accelerate adaptation. Strong heritable gene silencing leads to pre-adapted populations and interferes with mutation accumulation. It is possible that these non-mutant cells (orange cells) are epigenetically adapted. Chromosomes are represented by lines with telomeres (arrows), the *URA3* gene by green boxes and mutations by a red cross (either in the *URA3* gene, or outside to represent non-*URA3* mutations). The red shaded areas represent the regions of epigenetic gene silencing.

where a genetic change is beneficial only in the presence of an active epigenetic system. In other words, these mutations collaborate with epigenetic silencing as a means of increasing fitness.

Finally, we determined the means by which cells increase SIR-dependent 5-FOA resistance. The average degree of silencing in a population is dependent on the switching rate[25], which is the product of frequencies at which cells switch between the ON and OFF states. We determined the switching rate by pre-selecting cells to be in the *URA3*^{ON} state (by growth in medium lacking uracil) and then releasing them in the absence of selection. The rate at which cells reached an equilibrium between the *URA3*^{OFF} and *URA3*^{ON} states is a measure of the switching rate (see Supplementary Fig. 8 for raw data and fitted recovery curves). From these we estimated the *URA3*^{OFF} and *URA3*^{ON}rates as described in Methods. Interestingly, we found that the high, medium and low ancestral strains differed predominantly in the *URA3*^{OFF} rate (Fig. 3b). Strikingly, in the evolved clones analysed, we found that while the frequency of ON switching remained largely unchanged, cells showed an increase in the OFF rate of up to three to four orders of magnitude (as was the case for clones bearing mutations in *PPR1*). In these clones, cells spent more time in the silent state, indicating that evolved mutants resulted in enhanced silencing by modulating the frequency of OFF switching, rendering gene silencing more strongly heritable.

Discussion

Using a defined experimental evolution set-up in budding yeast, we minimized genetic variance and uniquely assessed the contribution of chromatin-based heritable gene silencing to adaptation in a selective environment. We show that multi-generational heritable gene expression through epigenetic chromatin states is a powerful contributor to driving of evolution. This is important because chromatin states impact directly on gene expression, which is a major source of phenotypic variation. We find that in our defined *URA3* reporter assay for tuneable heritable silencing, there is an optimal degree of silencing that accelerates adaptation (Fig. 4). Deviation from this results in either (1) clonal interference, where strongly silenced clones compete with de novo mutations, delaying their fixation, or (2) too little silencing, leading to insufficient mutational supply and extinction (Fig. 2).

We found that intermediate levels of silencing facilitate adaptation in two ways: first, the silencing phenotype resulted in an increase in the effective population size, aiding mutational supply (Fig. 2). This change in the tempo of adaptation appears to be a consequence of genetic assimilation of silencing through the accelerated acquisition of *ura*$^{-}$ mutations. Second, we found that the silencing machinery collaborated with several novel alleles, biasing the switching rate to the silent state and thus rendering the *URA3*^{OFF} state more stable (Fig. 3 and Supplementary Fig. 6). This changes the mode of adaptation by increasing capitalization of the mutational target on the silencing machinery. The genes we have identified are unlikely, per se, to be subject to silencing as these are distant from SIR-bound regions. Rather, they probably act by changing the degree of silencing at the telomere region.

Finally, we also found adapted populations in which no causative mutations could be found yet showed increased fitness. While a genetic change may have eluded us, it is an intriguing possibility that these clones adapted by purely epigenetic means. However, due to the relatively small increase in fitness, we cannot exclude the possibility that these clones are still in the ancestral state.

In sum, our findings may help explain how short-term epigenetic inheritance of transient gene expression states can have a long-lasting impact on adaptation, through mutation and the course of evolution. This is relevant because heritable gene expression is a widespread phenomenon in different organisms[36]. Among yeasts, there are around 350 naturally occurring genes within the range of subtelomeric gene silencing. Six per cent of these have been shown to be silenced in a SIR-dependent manner, and this percentage could be higher under stressful conditions[26]. Our results indicate that there may be an evolutionary advantage in maintaining particular genes within this region, since the epigenetic control of their expression may allow rapid adaptation to a novel stress. Furthermore, heritable control of gene expression could potentially buffer deleterious effects in a rapidly changing environment.

Methods

Strains and growth conditions. All *S. cerevisiae* strains used in this study (listed in Supplementary Fig. 9) were derived from S288c (*MATα*, *trpΔ63*, *hisΔ200*, *ura3-52*)[37]. LJY170, a *Ura*$^{+}$ strain, was created by restoring the endogenous *URA3* allele by integration of a *URA3* construct amplified from the strain FEP193, originally derived from pFEP24[22]. LJY181, a *ura*$^{-}$ strain, was created in which all *URA3* sequences were deleted by integration of a KanMX6 cassette amplified from pLJ32 (pLoxB-KMX) into LJY170, deleting nucleotides between positions 115,929 and 117,048 on chromosome V. The LJY170 *ura3* deleted strain was used for the integration of *URA3* cassettes at seven different positions in the subtelomeric region of the left arm of chromosome XI. Insertions were made telomere-proximal of the following nucleotide coordinates: position 1 (strain LJY182), 3,304; position 2 (strain LJY183), 2,804; position 3 (strain LJY184), 2,399; position 4 (strain LJY185), 1,623; position 5 (strain LJY186), 1,373; position 6 (strain LJY187), 1,123; position 7 (strain LJY188), 873. In all strains, *URA3* is transcribed in the telomere direction.

SIR3 knockout strains were constructed by replacing the whole open reading frame (between nucleotide positions 1,019,287 and 1,022,281 on chromosome XII) with a *hphMX4* cassette (hygromycin resistance) amplified from the plasmid pAG32[38]. *SIR3* was deleted in all seven strains bearing a telomeric *URA3* insertion (LJY182–LJY188), generating strains LJY189–LJY195, respectively (Supplementary Fig. 9).

All strains were maintained in either rich medium (yeast peptone dextrose; 1% Bacto yeast extract BD (Fisher, no. 212720), 2% peptone (Fisher, no. BP1420-500), 2% glucose (Merck, no. 1.08342.1000), either as liquid medium or supplemented with 2% agar (Roth, no. 2266,4) for solid medium) or complete synthetic dropout medium (CSM, 0.7% yeast nitrogen base (Sigma, no. Y0626), 0.1% CSM (MP Biomedicals, no. 4560-222), 0.005% tryptophan (Sigma, no. T0254), 0.002% histidine (Sigma, no. H8000), 0.001% uracil (Sigma, no. U0750), 2% glucose (Merck, no. 1.08342.1000), either as liquid medium or supplemented with 2% agar (Roth, no. 2266,4) for solid medium).

Spot assays. After 2 days of growth on rich yeast peptone dextrose media plates, fresh single colonies were picked and suspended in 100 µl of distilled, demineralized water. Six tenfold dilutions were prepared and 10 µl was plated onto either CSM or CSM supplemented with 0.1% 5-FOA (Apollo Scientific, no. PC4054), or onto plates that were additionally supplemented with 5 mM nicotinamide (Fisher, no. 1663C). Plates were imaged and scored after 3 days of incubation at 28 °C.

Growth curves. Cultures were grown in liquid yeast peptone dextrose at 28 °C for 16 h. Then, approximately 10^5 cells were diluted into 200 µl cultures of CSM supplemented with different concentrations of 5-FOA (0, 0.025, 0.05, 0.1%). Growth was monitored on a Bioscreen C system by measuring absorbance every 30 min.

Experimental evolution. All strains were pre-selected to be in the *URA3*$^+$ state by growing cells in liquid CSM lacking uracil for 16 h. Next, 10^6 cells were diluted in 1 ml liquid CSM supplemented with 0.05% 5-FOA. Every 24 h, absorbance was determined and 5×10^5 cells were transferred into fresh medium. If populations contained $<5\times10^5$ cells, these were considered extinct. At each passage, cells were analysed for viability, 5-FOA resistance and growth on medium lacking uracil (scoring *URA* state). For this, approximately one hundred cells were plated onto non-selective plates (yeast peptone dextrose or CSM) or at higher densities on plates containing 0.1% 5-FOA. Plates were incubated at 28 °C for 5 days, after which colonies were counted and cell numbers in each population estimated. The number of cells plated on non-selective media imposes a 1% threshold of detection for resistance. In some cases, a low number of epigenetically silenced cells were detected on plates with 5-FOA at time 0 h. Since these cells could not survive in medium lacking uracil during pre-selection, we assume these had arisen after plating due to their high frequency of switching. Plates with 5-FOA were replica-plated onto CSM plates lacking uracil and incubated for 3 days at 28 °C, after which the fractions of *ura*$^+$ and *ura*$^-$ clones in each population were estimated. Experiments were performed three times independently, with eight population replicates for each strain (a total of ≤24 replicates per strain across all experiments).

PCR analysis. To determine the frequency of recombination events that resulted in the deletion of the *URA3* gene relative to the frequency of point mutations or indels, we performed PCR analysis of the *ura*$^-$ evolved clones. We scored for the presence of the *URA3* locus with a primer within the *URA3* gene (sequence: ACTGGAGTTAGTTGAAGCATTAGGTC) matched with a primer outside the cassette in the telomere proximal region (sequence: ATCAACCTGTCTCCAAACCTAC). The absence of a PCR product is indicative of whole gene loss. The frequency of deletion events is then compared among all three yeast strains using Fisher's exact test with Bonferroni correction for multiple testing.

Sequencing. Representative evolved clones from classes *ura*$^+$ and *ura*$^-$ were isolated at the final time point (144 h), and genomic DNA was extracted using standard procedures based on bead lysis followed by phenol/chloroform extraction and ethanol precipitation of genomic DNA. Libraries were prepared with a Nextera kit (according to the manufacturer's instructions) and were sequenced at approximately 30X coverage using an Illumina MiSeq Sequencer. The reads were processed using SeqTK (github.com/lh3/seqtk) to trim low-quality reads. Alignment and mutation calling were performed by BreSeq[39] based on the yeast reference genome taken from the Yeast Genome Database (Saccharomyces Genome Database; www.yeastgenome.org). The alignments of all called mutations were manually checked. Mutations in homopolymers were discarded, because these are difficult to distinguish from sequencing errors and were all in intergenic regions. The list of mutations in each evolved clone was compared to that of mutations in its ancestor to determine which were acquired during the experiment. Whole-genome sequence data for all strains listed are available at the National Center for Biotechnology Information Sequence Read Archive, accession no. SRP129019.

Mutation rates. Mutation rates were determined by fluctuation tests and were performed on *sir3Δ* clones, as previously described[29]. Three clones per each position were analysed to account for possible inter-clonal differences. In brief, cultures were grown in CSM without uracil to saturation to select cells in the *URA3*$^+$ state. Cells were then transferred to 96 yeast peptone dextrose cultures at a concentration of 10^3cells ml^{-1}. After 3 days of non-selective growth, seven cultures were pooled and appropriate dilutions were plated on yeast peptone dextrose plates to estimate the average number of cells per well. The remaining 89 wells were plated as lawns onto CSM plates with 0.1% 5-FOA, to estimate the number of populations in which *ura*$^-$ mutations occurred. Plates were incubated at 28 °C for 5 days, after which the number of mutants per lawn was scored. The mutation rates were calculated using the p0 method[40], and 95% confidence intervals were determined with the exact binomial test. For SIR3$^+$ clones, the same procedure was performed except that the CSM plates with 0.1% 5-FOA were supplemented with 5 mM nicotinamide to prevent silencing.

Growth rates of evolved clones. Cells were maintained for several passages in yeast peptone dextrose without selection. These were then diluted in CSM supplemented with 0.05% 5-FOA, and growth was monitored using a Bioscreen C set-up. The time elapsed in exponential phase between absorbance 0.1 and 0.6 was determined. This ensures that any non-linearity between absorbance and cell number affects all strains in the same way. Growth rate was calculated as $\log_2$ of fold differences in absorbance per unit time.

Determination of switching rates. To determine the epigenetic switching rates we used a method analogous to that described previously[23]. All clones (ancestral and evolved) were pre-selected to be in the *URA3*^{ON} state by growing cells for 16 h in liquid CSM lacking uracil. Then, four independent cultures were prepared by placing 10^6 cells into fresh non-selective media (CSM containing 0.002% of uracil). The populations were sampled at given time points (0, 8, 24, 32, 48, 56, 72 and 80 h) and plated on CSM with 0.1% 5-FOA to score for 5-FOA resistance. The rise in frequency of resistance to the selective drug is a measure of the acquisition of epigenetic silencing of the *URA3* gene. The dynamics of the increase in the frequency of resistance (f_r) are dependent on the rate of conversion from active to epigenetically silenced state (μ_{OFF}) and the rate of conversion from silenced to an active state (μ_{ON}) of the gene. Under such a model the change in the frequency of resistant cells is given by:

$$\frac{df_r(t)}{dt} = \mu_{OFF}*(1 - f_r(t)) - \mu_{ON}*f_r(t)$$

By solving this differential equation in Mathematica (using DSolve) we obtained:

$$f_r(t) = \frac{e^{-t*\mu_{OFF}-t*\mu_{ON}}*(-1+e^{t*(\mu_{ON}+\mu_{OFF})})*\mu_{OFF}}{\mu_{OFF}+\mu_{ON}}$$

We performed a non-linear fit of this formula to the frequencies of resistance over time and extracted the values for μ_{OFF} and μ_{ON}, as well as the 95% confidence intervals (Mathematica NonlinearModelFit).

Statistical analysis. Fisher's exact test, binomial test, analysis of variance (ANOVA) and Tukey's honestly significant difference were performed using the standard command line in R software[41], with default parameters. The log-rank test was performed using GraphPad. Significance in differences of growth rate between evolved and ancestral clones was determined using pairwise *t*-test with Bonferroni correction for multiple testing.

Reporting Summary. Further information on experimental design is available in the Nature Research Reporting Summary linked to this article.

Data availability

Whole-genome sequence data for all strains listed in Supplementary Fig. 6 are available at the National Center for Biotechnology Information Sequence Read Archive, accession no. SRP129019.

Received: 19 April 2018; Accepted: 10 December 2018;
Published online: 04 February 2019

References

1. Johannes, F. et al. Assessing the impact of transgenerational epigenetic variation on complex traits. *PLoS Genet.* **5**, e1000530 (2009).
2. Cortijo, S. et al. Mapping the epigenetic basis of complex traits. *Science* **343**, 1145–1148 (2014).
3. Heard, E. & Martienssen, R. A. Transgenerational epigenetic inheritance: myths and mechanisms. *Cell* **157**, 95–109 (2014).
4. Simpson, G. G. The Baldwin effect. *Evolution* **7**, 110 (1953).
5. Waddington, C. H. Canalization of development and genetic assimilation of acquired characters. *Nature* **183**, 1654–1655 (1959).
6. Lande, R. Adaptation to an extraordinary environment by evolution of phenotypic plasticity and genetic assimilation. *J. Evol. Biol.* **22**, 1435–1446 (2009).
7. Cowen, L. E. & Lindquist, S. Hsp90 potentiates the rapid evolution of new traits: drug resistance in diverse fungi. *Science* **309**, 2185–2189 (2005).
8. Jarosz, D. F. & Lindquist, S. Hsp90 and environmental stress transform the adaptive value of natural genetic variation. *Science* **330**, 1820–1824 (2010).
9. True, H. L. & Lindquist, S. L. A yeast prion provides a mechanism for genetic variation and phenotypic diversity. *Nature* **407**, 477–483 (2000).
10. Halfmann, R. et al. Prions are a common mechanism for phenotypic inheritance in wild yeasts. *Nature* **482**, 363–368 (2012).
11. Klosin, A., Casas, E., Hidalgo-Carcedo, C., Vavouri, T. & Lehner, B. Transgenerational transmission of environmental information in C. elegans. *Science* **356**, 320–323 (2017).

12. Daxinger, L. & Whitelaw, E. Understanding transgenerational epigenetic inheritance via the gametes in mammals. *Nat. Rev. Genet.* **13**, 153–162 (2012).
13. Bonduriansky, R. & Day, T. Nongenetic inheritance and its evolutionary implications. *Annu. Rev. Ecol. Evol. Syst.* **40**, 103–125 (2009).
14. Klironomos, F. D., Berg, J. & Collins, S. How epigenetic mutations can affect genetic evolution: model and mechanism. *Bioessays* **35**, 571–578 (2013).
15. Kronholm, I. & Collins, S. Epigenetic mutations can both help and hinder adaptive evolution. *Mol. Ecol.* **25**, 1856–1868 (2016).
16. Charlesworth, D., Barton, N. H. & Charlesworth, B. The sources of adaptive variation. *Proc. Biol. Sci.* **284**, 20162864 (2017).
17. Rine, J. & Herskowitz, I. Four genes responsible for a position effect on expression from HML and HMR in *Saccharomyces cerevisiae*. *Genetics* **116**, 9–22 (1987).
18. Aparicio, O. M., Billington, B. L. & Gottschling, D. E. Modifiers of position effect are shared between telomeric and silent mating-type loci in *S. cerevisiae*. *Cell* **66**, 1279–1287 (1991).
19. Ivy, J. M., Klar, A. J. & Hicks, J. B. Cloning and characterization of four SIR genes of *Saccharomyces cerevisiae*. *Mol. Cell. Biol.* **6**, 688–702 (1986).
20. Imai, S., Armstrong, C. M., Kaeberlein, M. & Guarente, L. Transcriptional silencing and longevity protein Sir2 is an NAD-dependent histone deacetylase. *Nature* **403**, 795–800 (2000).
21. Moazed, D. Mechanisms for the inheritance of chromatin states. *Cell* **146**, 510–518 (2011).
22. Pryde, F. E. & Louis, E. J. Limitations of silencing at native yeast telomeres. *EMBO J.* **18**, 2538–2550 (1999).
23. Jeffery, D. C. B. et al. Analysis of epigenetic stability and conversions in *Saccharomyces cerevisiae* reveals a novel role of CAF-I in position-effect variegation. *Nucleic Acids Res.* **41**, 8475–8488 (2013).
24. Boeke, J. D., Trueheart, J., Natsoulis, G. & Fink, G. R. 5-Fluoroorotic acid as a selective agent in yeast molecular genetics. *Meth. Enzymol.* **154**, 164–175 (1987).
25. Gottschling, D. E., Aparicio, O. M., Billington, B. L. & Zakian, V. A. Position effect at *S. cerevisiae* telomeres: reversible repression of Pol II transcription. *Cell* **63**, 751–762 (1990).
26. Ellahi, A., Thurtle, D. M. & Rine, J. The chromatin and transcriptional landscape of native *Saccharomyces cerevisiae* telomeres and subtelomeric domains. *Genetics* **200**, 505–521 (2015).
27. Gerrish, P. J. & Lenski, R. E. The fate of competing beneficial mutations in an asexual population. *Genetica* **102-103**, 127–144 (1998).
28. Batté, A. et al. Recombination at subtelomeres is regulated by physical distance, double-strand break resection and chromatin status. *EMBO J.* **36**, 2609–2625 (2017).
29. Lang, G. I. & Murray, A. W. Estimating the per-base-pair mutation rate in the yeast *Saccharomyces cerevisiae*. *Genetics* **178**, 67–82 (2008).
30. Lang, G. I. & Murray, A. W. Mutation rates across budding yeast chromosome VI are correlated with replication timing. *Genome Biol. Evol.* **3**, 799–811 (2011).
31. Ricchetti, M., Dujon, B. & Fairhead, C. Distance from the chromosome end determines the efficiency of double strand break repair in subtelomeres of haploid yeast. *J. Mol. Biol.* **328**, 847–862 (2003).
32. Renauld, H. et al. Silent domains are assembled continuously from the telomere and are defined by promoter distance and strength, and by SIR3 dosage. *Genes Dev.* **7**, 1133–1145 (1993).
33. Aparicio, O. M. & Gottschling, D. E. Overcoming telomeric silencing: a trans-activator competes to establish gene expression in a cell cycle-dependent way. *Genes Dev.* **8**, 1133–1146 (1994).
34. Zhou, J., Zhou, B. O., Lenzmeier, B. A. & Zhou, J.-Q. Histone deacetylase Rpd3 antagonizes Sir2-dependent silent chromatin propagation. *Nucleic Acids Res.* **37**, 3699–3713 (2009).
35. Bitterman, K. J., Anderson, R. M., Cohen, H. Y., Latorre-Esteves, M. & Sinclair, D. A. Inhibition of silencing and accelerated aging by nicotinamide, a putative negative regulator of yeast sir2 and human SIRT1. *J. Biol. Chem.* **277**, 45099–45107 (2002).
36. Youngson, N. A. & Whitelaw, E. Transgenerational epigenetic effects. *Annu. Rev. Genomics Hum. Genet.* **9**, 233–257 (2008).
37. Mortimer, R. K. & Johnston, J. R. Genealogy of principal strains of the yeast genetic stock center. *Genetics* **113**, 35–43 (1986).
38. Goldstein, A. L. & McCusker, J. H. Three new dominant drug resistance cassettes for gene disruption in *Saccharomyces cerevisiae*. *Yeast* **15**, 1541–1553 (1999).
39. Deatherage, D. E. & Barrick, J. E. Identification of mutations in laboratory-evolved microbes from next-generation sequencing data using breseq. *Methods Mol. Biol.* **1151**, 165–188 (2014).
40. Rosche, W. A. & Foster, P. L. Determining mutation rates in bacterial populations. *Methods* **20**, 4–17 (2000).
41. R Core Team. *R: A Language and Environment for Statistical Computing* (R Foundation for Statistical Computing, Vienna, 2013).

Acknowledgements

We thank R. Kolodner (University of California, San Diego) and E. Louis (University of Leicester) for strains, and I. Gordo, P. Beldade, C. Bank, M. Ferreira (all Instituto Gulbenkian de Ciência), L.-M. Chevin (Centre National de la Recherche Scientifique, Montpellier) and T. Flatt (University of Fribourg) for helpful comments and suggestions. We acknowledge the Instituto Gulbenkian de Ciência Gene Expression Unit for genome sequencing support. Salary support to D.S. was provided by the Fundação para a Ciência e a Tecnologia fellowship (no. SFRH/BD/52170/2013), and Investigador FCT positions to L.P. and L.E.T.J. This work was supported by the Instituto Gulbenkian de Ciência.

Author contributions

D.S., L.P. and L.J. conceived the study and designed the experiments. D.S. constructed the strains and performed the experiments. D.S., L.P. and L.J. critically analysed the data. D.S. and L.J. created the figures. D.S., L.P. and L.J. wrote the manuscript. L.P. and L.J. provided resources, funding and supervision.

Competing interests

The authors declare no competing interests.

Additional information

Supplementary information is available for this paper at https://doi.org/10.1038/s41559-018-0781-2.

Correspondence and requests for materials should be addressed to L.P. or L.E.T.J.

nature ecology & evolution

SUPPLEMENTARY INFORMATION

https://doi.org/10.1038/s41559-018-0781-2

In the format provided by the authors and unedited.

Epigenetic gene silencing alters the mechanisms and rate of evolutionary adaptation

Dragan Stajic[1], Lília Perfeito[1*] and Lars E. T. Jansen[1,2*]

[1]Instituto Gulbenkian de Ciência, Oeiras, Portugal. [2]Department of Biochemistry, University of Oxford, Oxford, UK. *e-mail: lperfeito@igc.gulbenkian.pt; lars.jansen@bioch.ox.ac.uk

Supplemental information for "Epigenetic gene silencing alters the mechanisms and rate of evolutionary adaptation"

Dragan Stajic, Lília Perfeito and Lars E.T Jansen

Supplemental Information consists of 9 Supplemental figures.

Figure S1

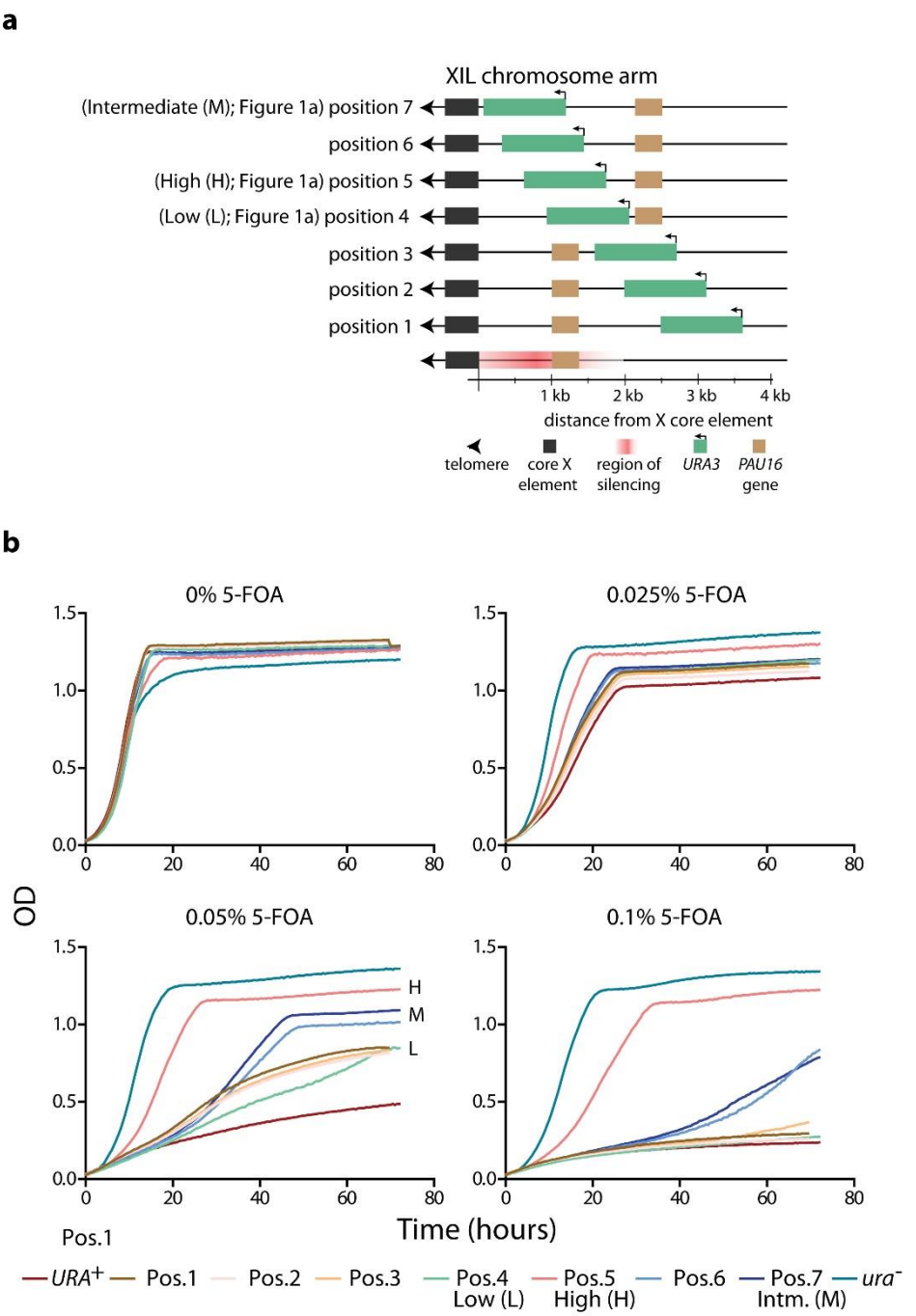

Figure S1.Titration of 5-FOA selection for evolution experiments. a. Scheme depicting 7 different insertion positions of the *URA3* gene cassette relative to the core X element near the telomere on the left arm of chromosome XI (see Figure S9 for strain details). The *URA3* positions representing High (H), Medium (M) and Low (L) silencing that are used for further experiments and shown in Figure 1 are indicated. **b.** Strains with uniquely positioned *URA3* insertions were grown in indicated concentration of 5-FOA. Growth was monitored using a Bioscreen C setup to obtain real-time growth curves at 30 minute intervals. Data was obtained for 9 replicate cultures per strain (of which one representative population is shown for clarity). The positions representing High (H), Medium (M) and Low (L) silencing are indicated in the 0.05% 5-FOA condition which is used for subsequent experimental evolution experiments.

Figure S2 - page 1

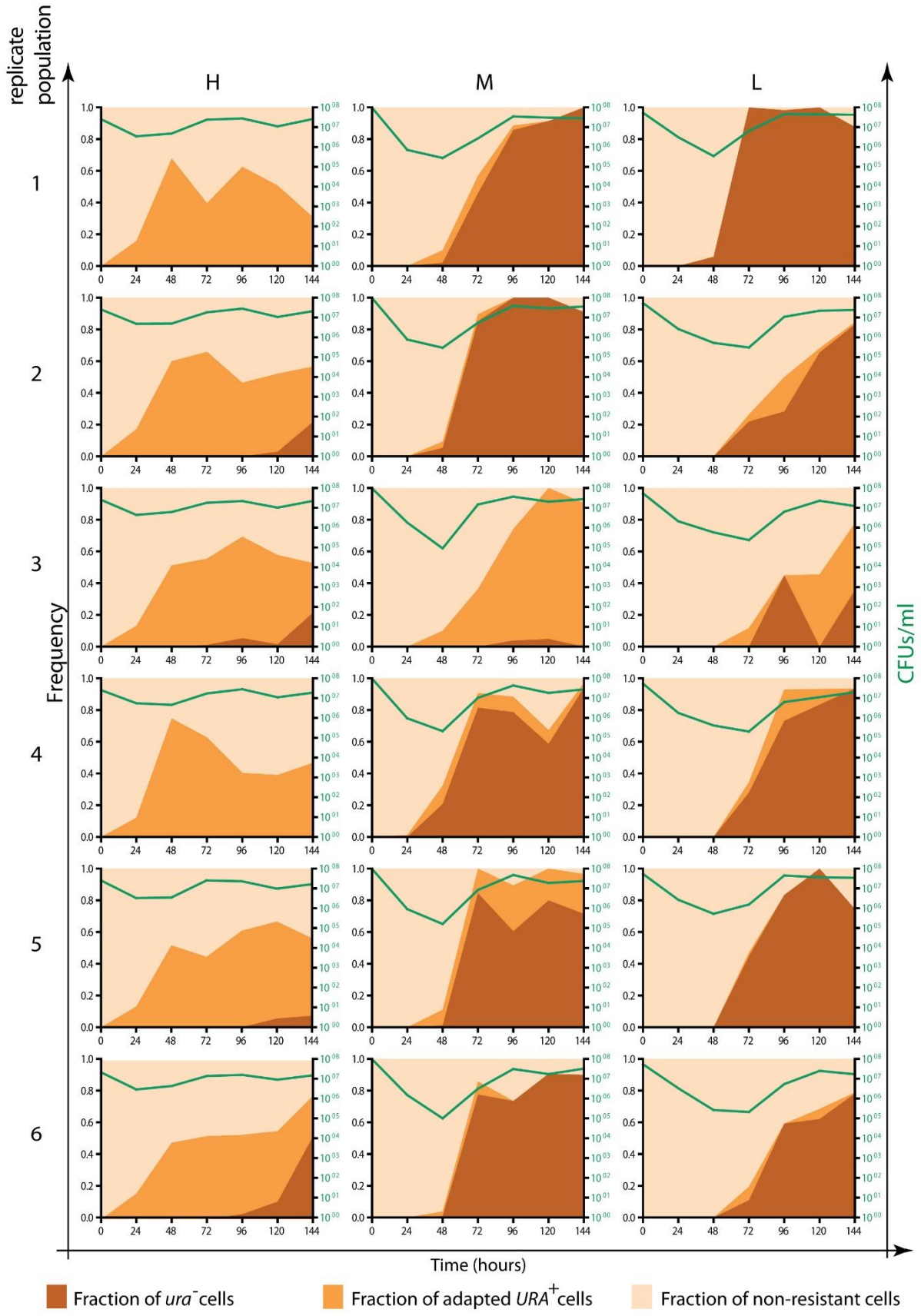

Figure S2 - page 2

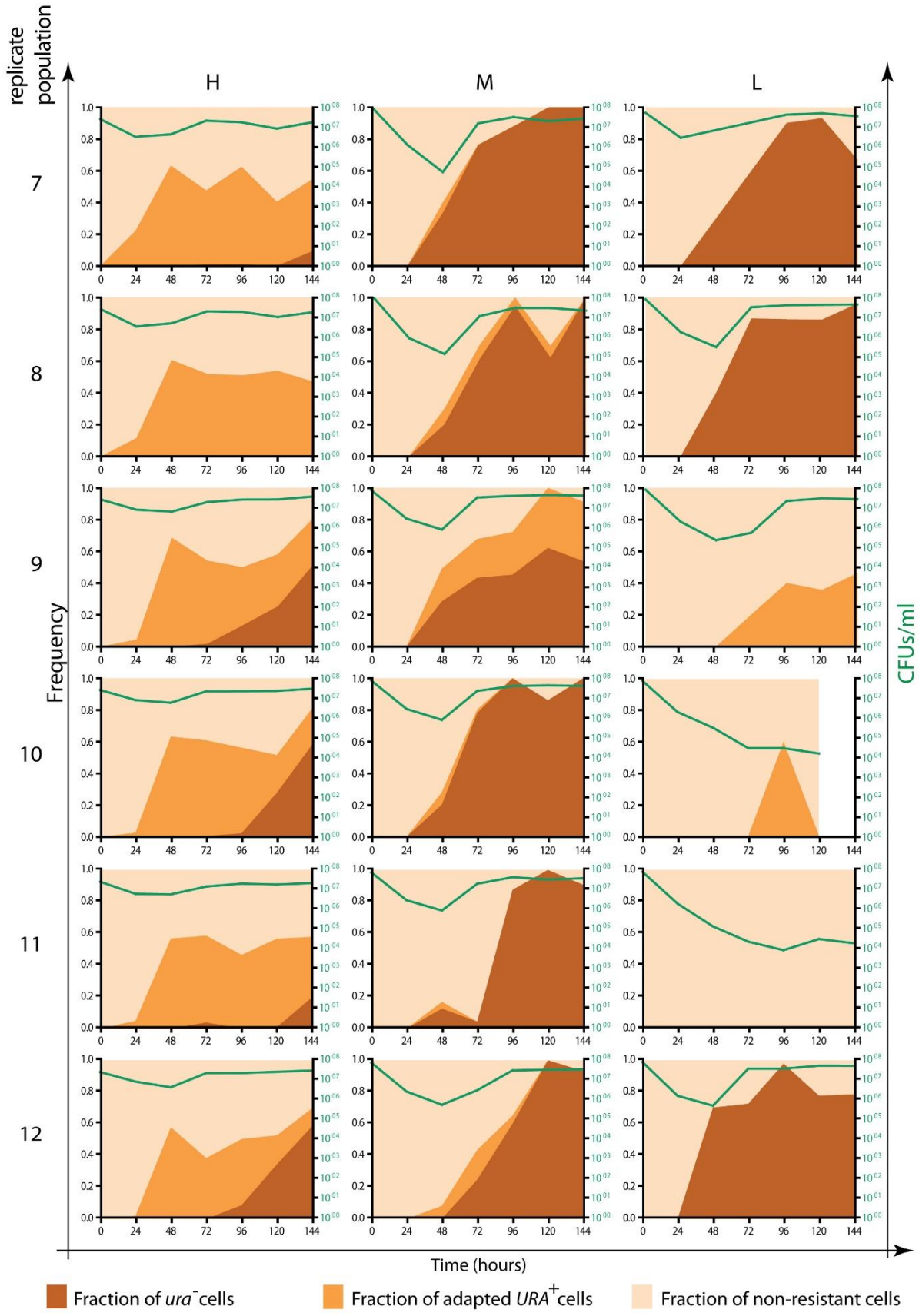

Figure S2 - page 3

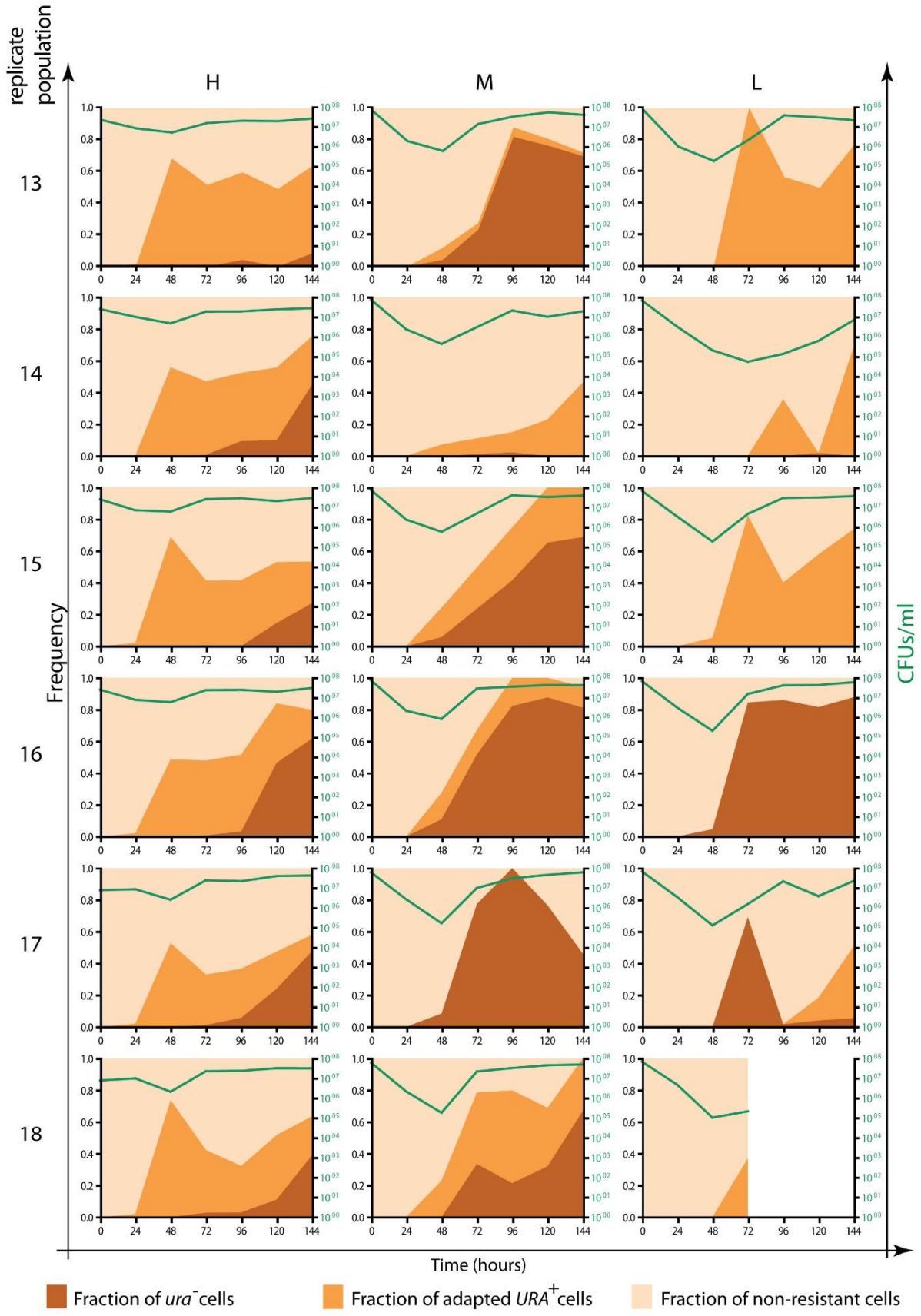

Figure S2 - page 4

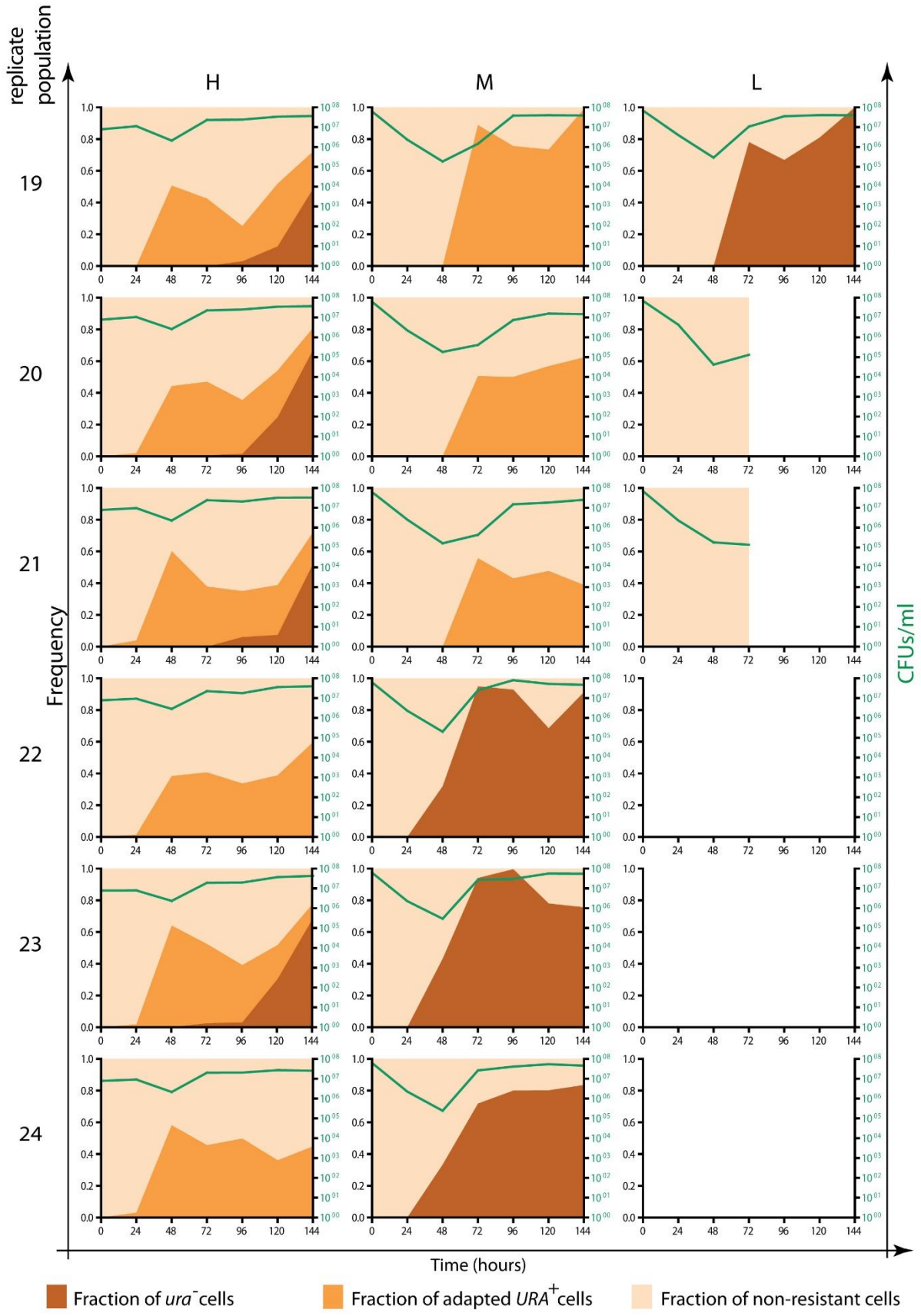

Figure S2 (4 pages). Population dynamics of acquisition of 5-FOA resistance during experimental evolution. Plots as shown in Figure 2b and c. All 24 replicate populations are shown (H- 24 replicates, M- 24 replicates, L- 21 replicate). Green line indicates the total number of living cells within a population during the course of the experiment [colony forming units (CFUs)/ml]. Colours represent the different phenotypic subgroups within each population (as indicated), plotted as the size fraction of each subgroup within the total population across time.

Figure S3 - page 1

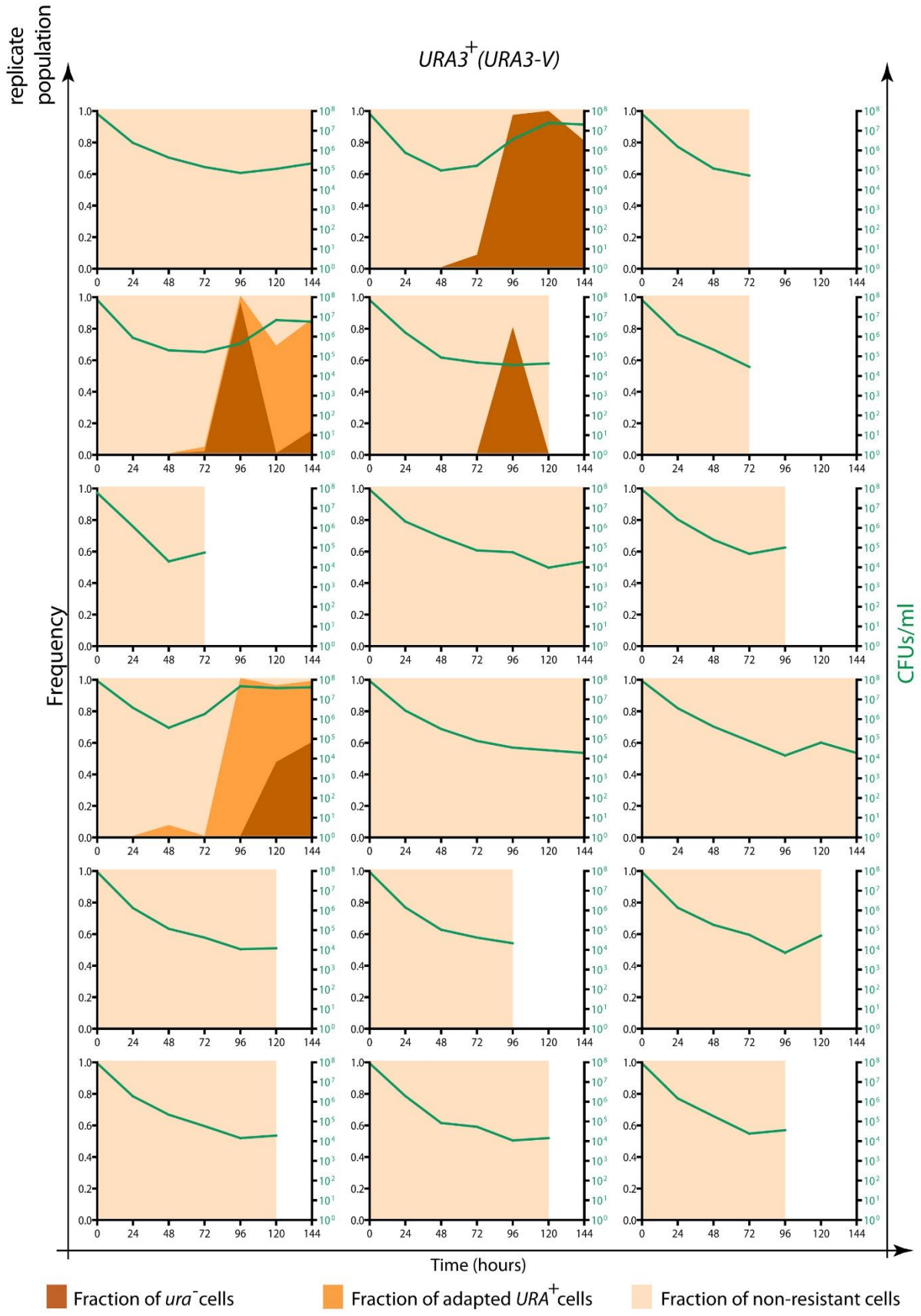

Figure S3 - page 2

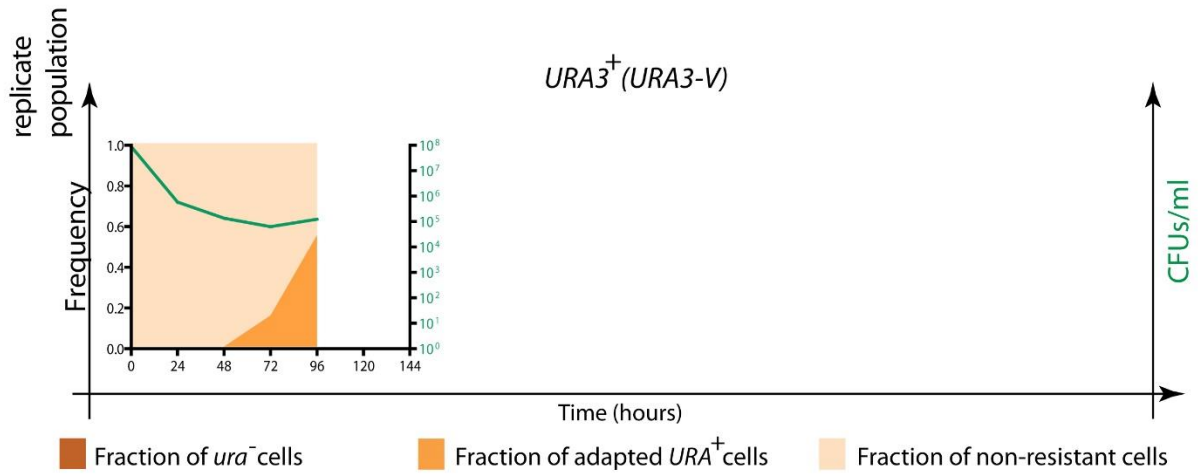

Figure S3 (2 pages). Population dynamics of acquisition of 5-FOA resistance during experimental evolution of wild type strain (*URA3* gene at unlinked non-telomeric position on chromosome V, non-silenced). Plots as shown in Figure 2b and c. 19 replicate wildtype (strain LJY170, see Figure S9) populations are shown. Green line indicates the total number of living cells within a population during the course of the experiment [colony forming units (CFUs)/ml]. Colours represent the different phenotypic subgroups within each population (as indicated), plotted as the size fraction of each subgroup within the total population across time.

Figure S4 - page 1

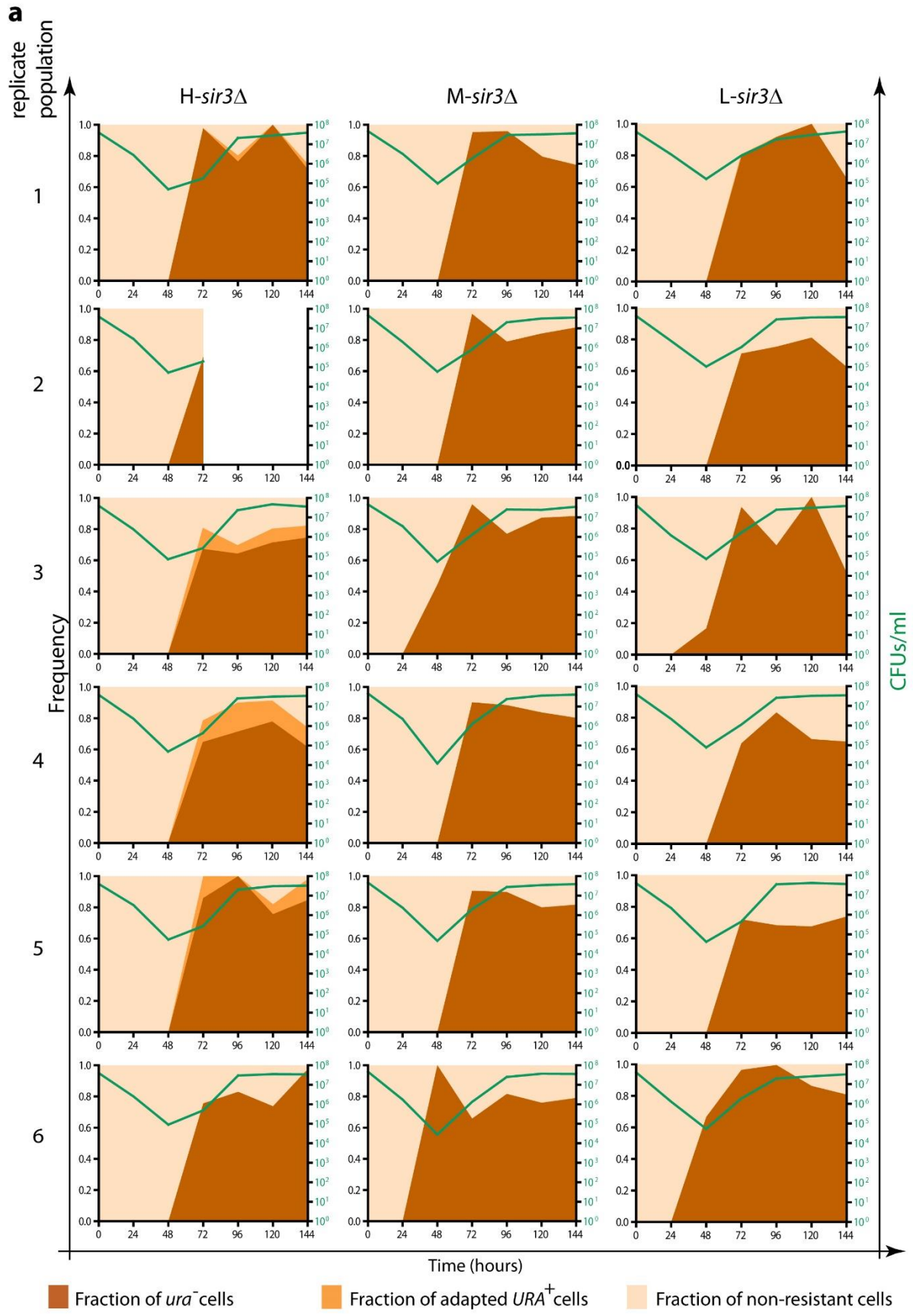

Figure S4 - page 2

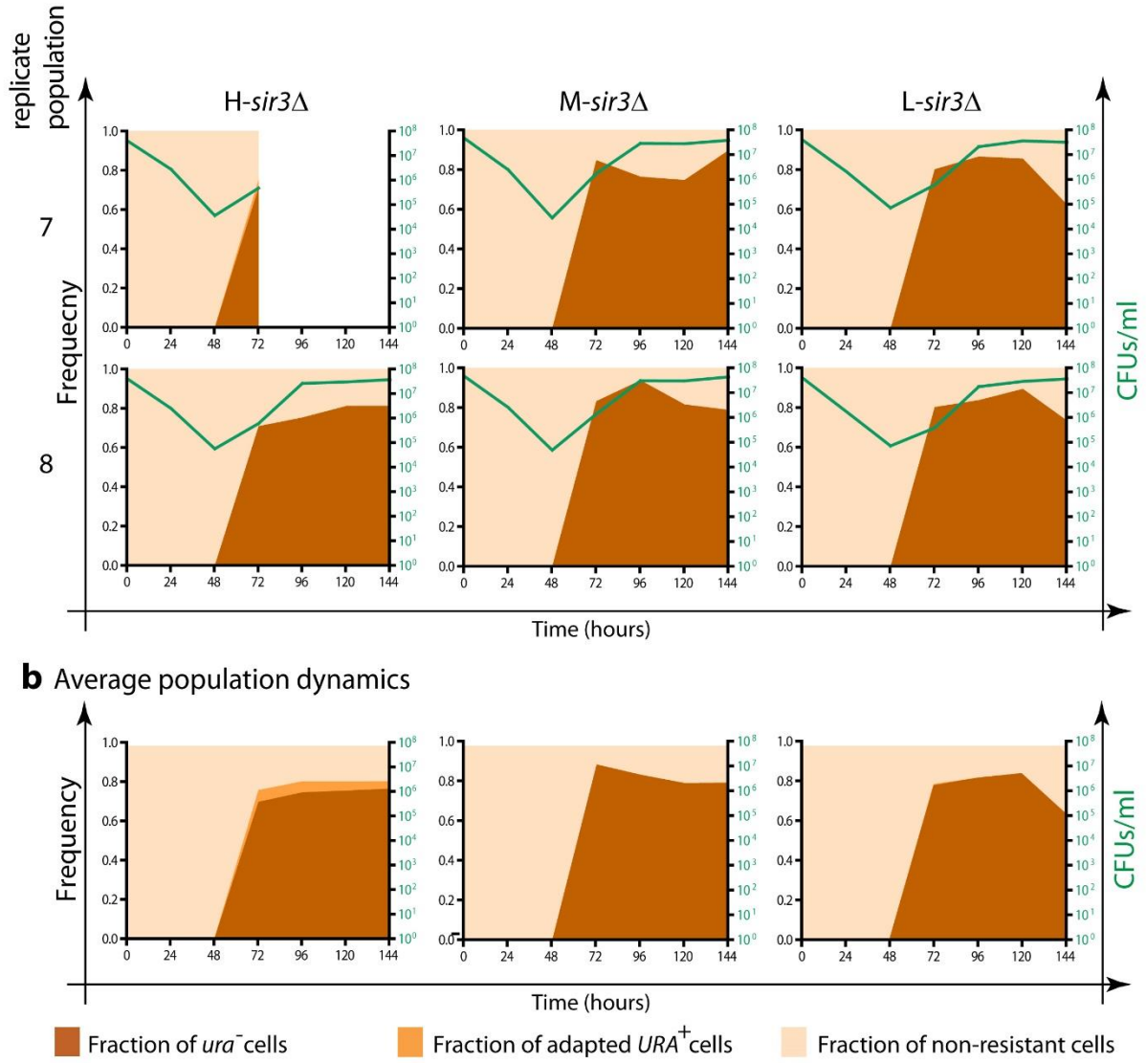

Figure S4 (2 pages). Population dynamics of acquisition of 5-FOA resistance during experimental evolution in *sir3Δ* mutants. a. Plots as shown in Figure 2b and c. For *H-sir3Δ, M-sir3Δ and L-sir3Δ* (strains LJY193, LJY195 and LJY192, respectively, see Figure S9). 8 replicate populations for each strain are shown. Green line indicates the total number of living cells within a population during the course of the experiment [colony forming units (CFUs)/ml]. Colours represent the different phenotypic subgroups within each population (as indicated), plotted as the size fraction of each subgroup within the total population across time. **b**. Median values of 8 replicate evolution experiments.

Figure S5

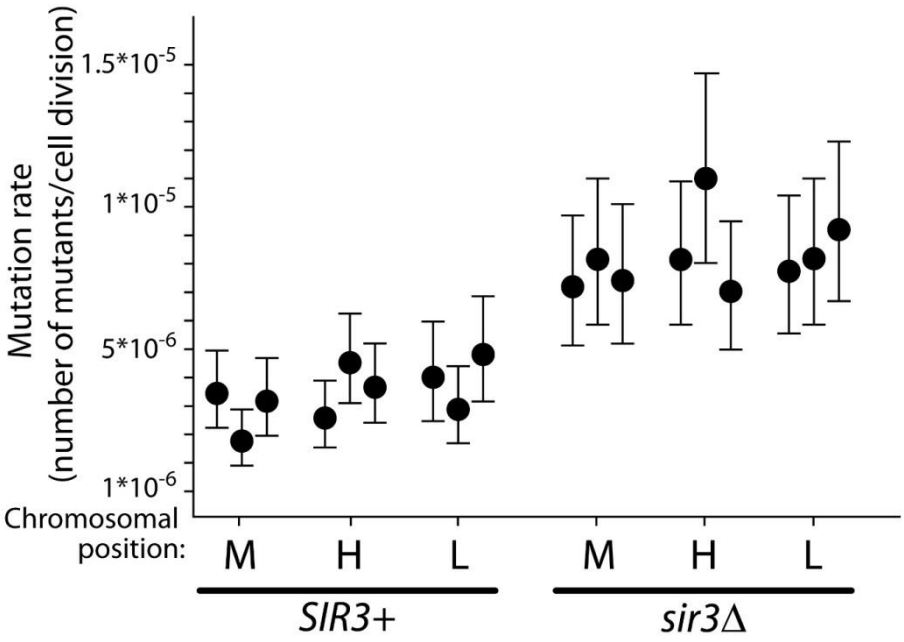

Figure S5. Comparable intrinsic mutation rates at different *URA3* positions at telomere of XI-L. Fluctuation tests were performed for indicated *URA3* positions in a *sir3Δ* or *SIR3*+ background. Mutations were allowed to accumulate in the absence of selection and were then scored on 5-FOA. For *SIR3*+ strains scoring of mutations was performed in the presence of 5-FOA + nicotinamide (NAM) to avoid 5-FOA resistance due to silencing. Three independent clones were analysed for each position. The mutation rate was estimated using the p0 method[40]. Calculated rate is plotted for each experiment and 95% confidence interval was determined using binomial exact test (shown as whiskers).

Figure S6

Evolved non-switching *ura-* clones									
Strain	**Clone**	**Repl. Pop.**	**Chrom.**	**Position**	**ances. allele**	**evol. allele**	**Type**	**Gene**	**AA change**
Pos.7-M	6M-3	6	XI	1-1,012			deletion containing *URA3*		
Pos.7-M	8M-3	8	XI	1-1,335			deletion containing *URA3*		
Pos.7-M	3M-7	11	XI	1-2,645			deletion containing *URA3*		
Pos.7-M	8M-7	16	XI	1-2,343			deletion containing *URA3*		
Pos.7-M	5M-9	21	XI	1-1,550			deletion containing *URA3*		
Pos.7-M	1M-9	17	XI	1-1,592			deletion containing *URA3*		
Pos.5-H	2M-3	2	XI	1-2,405			deletion containing *URA3*		
Pos.5-H	5M-3	5	XI	1-2,348			deletion containing *URA3*		
Pos.5-H	3M-7	11	XI	1-1,356			deletion containing *URA3*		
Pos.5-H	4M-7	12	XI	1-2,552			deletion containing *URA3*		
Pos.5-H	4M-9	20	XI	1-1,356			deletion containing *URA3*		
Pos.5-H	1M-9	17	V	116.293	G	T	Nonsynonymous	*URA3*	E>stop
Pos.5-H	1M-9	17	XV	124.046	C	A	Nonsynonymous	*ITR2*	L>I
Pos.4-L	1M-7	1	V	116.795			1bp deletion	*URA3*	
Pos.4-L	5M-7	5	XI	1-2,407			deletion containing *URA3*		
Pos.4-L	8M-7	7	XI	1-1,696			deletion containing *URA3*		
Pos.4-L	1M-9	8	XI	1-1,597			deletion containing *URA3*		
Pos.4-L	7M-9	12	XI	1-2,180			deletion containing *URA3*		

Evolved silent but switchable *URA+* clones									
Strain	**Clone**	**Repl. Pop.**	**Chrom.**	**Position**	**ances. allele**	**evol. allele**	**Type**	**Gene**	**AA change**
Pos.7-M	3E-3	3	XII	173.691	A	C	Nonsynonymous	*PPR1*	L>stop
Pos.7-M	8E-3	8	XIV	18.043	A	C	Nonsynonymous	*RPD3*	Y>stop
Pos.7-M	6E-7	14	XVI	185.419	T	G	Nonsynonymous	*NAB3*	N>T
Pos.7-M	6E-7	14	XVI	1,032,708	C	G	Nonsynonymous	*GPB1*	G>A
Pos.7-M	8E-7	16	XII	173.179	C	A	Nonsynonymous	*PPR1*	E>stop
Pos.7-M	4E-9	20					no mutation		
Pos.7-M	5E-9	21					no mutation		
Pos.5-H	1E-3	1					no mutation		
Pos.5-H	5E-3	5					no mutation		
Pos.5-H	3E-7	11					no mutation		
Pos.5-H	4E-7	12					no mutation		
Pos.5-H	1E-9	17					no mutation		
Pos.5-H	4E-9	20					no mutation		
Pos.4-L	2E-7	2	IV	1,247,059	G	A	Nonsynonymous	*MUS81*	A>T
Pos.4-L	2E-7	2	XII	638.857	T	C	Nonsynonymous	*YEF3*	L>S
Pos.4-L	4E-7	4					no mutation		
Pos.4-L	7E-7	6					no mutation		
Pos.4-L	3E-7	3	XII	638.857	T	C	Nonsynonymous	*YEF3*	L>S
Pos.4-L	3E-9	9	XII	173.515	T	A	Nonsynonymous	*PPR1*	R>stop
Pos.4-L	3E-9	9	XI	575.988	T	C		intergenic	

Figure S6. Silenced strains evolve by expanding the mutational target. Whole genome sequencing identifies mutations in evolved clones. For each *URA3* position 10-12 evolved clones were isolated at the end of the 144 hour experiment. Both *ura*$^-$ and silenced (5-FOA resistant but switchable) *ura*$^+$ clones were analysed. In evolved *ura*$^-$ clones, deletion of the telomere end containing *URA3* was the dominant mutational event. In evolved clones that increased 5-FOA resistances but maintained the capacity to switch, novel mutational targets were identified. Evolved clones from *URA3*-M (blue), *URA3*-H (green) and *URA3*-L (magenta) are colour coded corresponding to the graphs in Figure 3.

Figure S7

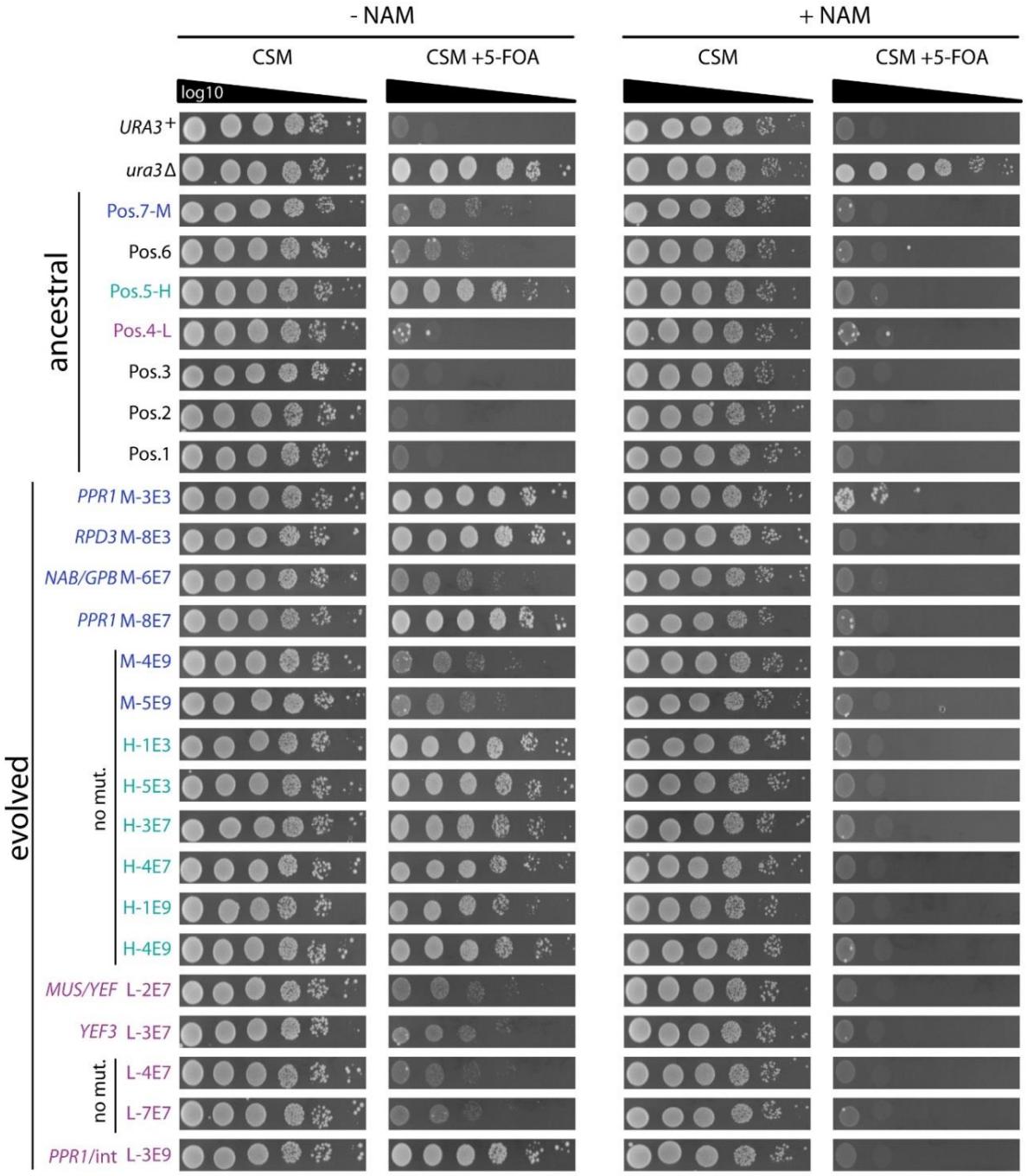

Figure S7. Non-*URA3* mutations in silenced strains genetically interact with the silencing machinery. Nicotinamide abolishes 5-FOA resistance in the adapted *URA3*$^{+}$ silenced clones. Ten-fold dilutions of indicated ancestral and evolved clones were spotted on plates containing nicotinamide (NAM; with and without 5-FOA) or minimal media plates (CSM-with and without 5-FOA) to control for the level of resistance to the 5-FOA. *ura3Δ* (LJY181) and *URA3*$^{+}$ (LJY170) strains were used as positive and negative controls respectively. Corresponding mutations for each evolved clone are indicated. Note that at high cell densities, few breakthrough colonies appear. We confirmed these to be *ura-* clones appearing due to large cell numbers in correspondence with the mutation frequency determined in Figure S5.

Figure S8

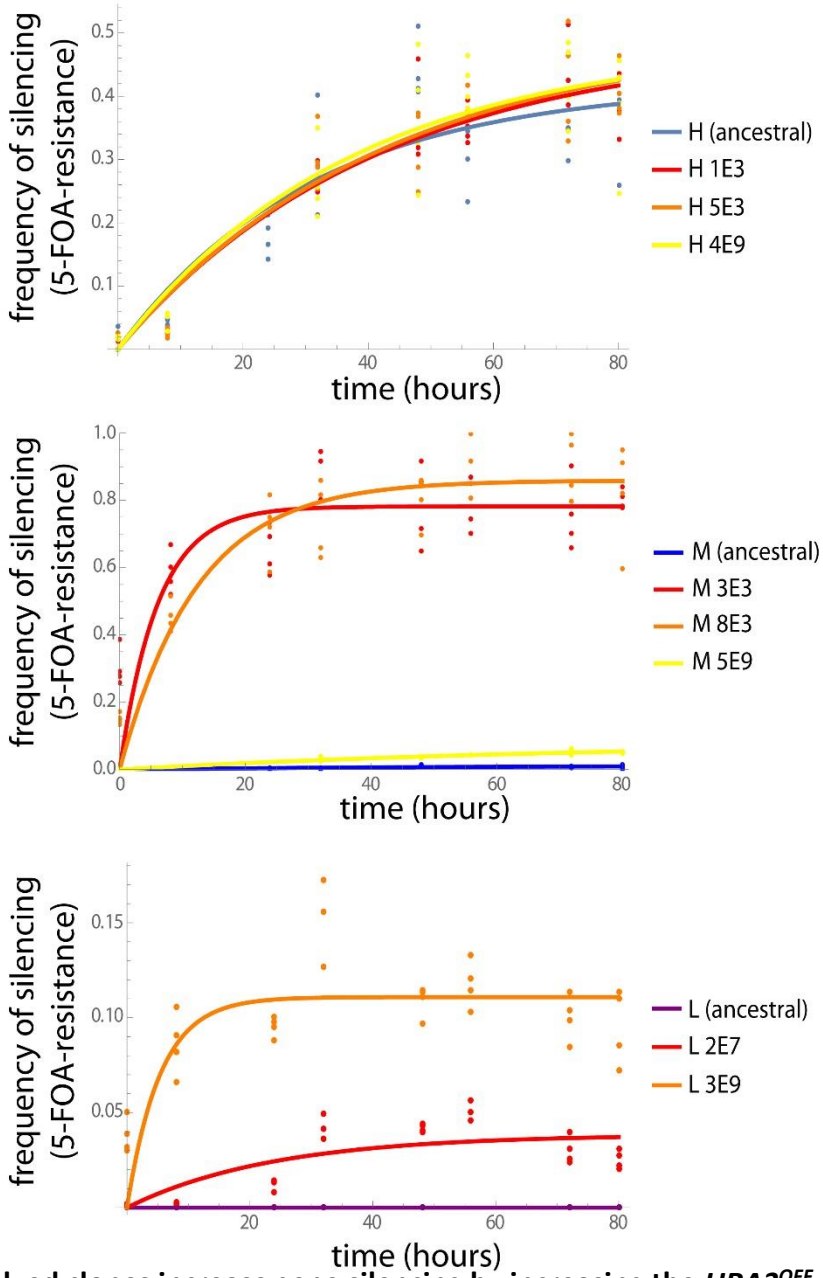

Figure S8. Evolved clones increase gene silencing by increasing the *URA3^{OFF}* rate. Switching rate assay: Ancestral strains and the indicated derivative evolved clones were preselected on medium lacking Uracil (all *URA3^{on}*) and released into non-selective medium. At indicated time points, cells were plated on 0.1% 5-FOA to score for the fraction of 5-FOA resistant clones (as a measure of the degree of silencing). 4 replicate experiments are shown for each strain and data was fitted to estimate the *URA3^{on}* and *URA3^{off}* rates (see methods). Note that the following data points were omitted from the analysis due to low colony count at these time points: M-(ancestral) at 56h; H-evolved strains and M-5E9 at 24h. The R-squared values of the data fitting for each clone is as follows: M-ancestral: 0.82, H-ancestral: 0.94, L-ancestral: 0.88, H-1E3: 0.97, H-5E3: 0.92, H-4E9: 0.96, M-3E3: 0.96, M-8E3: 0.97, M-5E9: 0.97, L-2E7: 0.85, L-3E9: 0.94.

Figure S9

strain nr.	background	genotype	relevant mutation	reference
LJY6	*S288C*	*MATa trpΔ63, hisΔ200, ura3-52*		*37*
LJY170	*S288C*	*MATa trpΔ63, hisΔ200*	*reconstituted URA3 gene*	*this study, derived from LJY6*
LJY181	*S288C*	*MATa trpΔ63, hisΔ200, ura3Δ::KanMX6*	*replacing URA3 with KanMX6*	*this study, derived from LJY170*
LJY182	*S288C*	*MATa trpΔ63, hisΔ200, ura3Δ::KanMX6, TEL-XIL::URA3*	*URA3 at position 3304 of Chrom XIL (pos.1)*	*this study, derived from LJY181*
LJY183	*S288C*	*MATa trpΔ63, hisΔ200, ura3Δ::KanMX6, TEL-XIL::URA3*	*URA3 at position 2804 of Chrom XIL (pos.2)*	*this study, derived from LJY181*
LJY184	*S288C*	*MATa trpΔ63, hisΔ200, ura3Δ::KanMX6, TEL-XIL::URA3*	*URA3 at position 2399 of Chrom XIL (pos.3)*	*this study, derived from LJY181*
LJY185	*S288C*	*MATa trpΔ63, hisΔ200, ura3Δ::KanMX6, TEL-XIL::URA3*	*URA3 at position 1623 of Chrom XIL (pos.4)*	*this study, derived from LJY181*
LJY186	*S288C*	*MATa trpΔ63, hisΔ200, ura3Δ::KanMX6, TEL-XIL::URA3*	*URA3 at position 1373 of Chrom XIL (pos.5)*	*this study, derived from LJY181*
LJY187	*S288C*	*MATa trpΔ63, hisΔ200, ura3Δ::KanMX6, TEL-XIL::URA3*	*URA3 at position 1123 of Chrom XIL (pos.6)*	*this study, derived from LJY181*
LJY188	*S288C*	*MATa trpΔ63, hisΔ200, ura3Δ::KanMX6, TEL-XIL::URA3*	*URA3 at position 873 of Chrom XIL (pos.7)*	*this study, derived from LJY181*
LJY189	*S288C*	*MATa trpΔ63, hisΔ200, ura3Δ::KanMX6, sir3Δ::HYG, TEL-XIL::URA3*	*URA3 at position 3304 of Chrom XIL (pos.1)*	*this study, derived from LJY182*
LJY190	*S288C*	*MATa trpΔ63, hisΔ200, ura3Δ::KanMX6, sir3Δ::HYG, TEL-XIL::URA3*	*URA3 at position 2804 of Chrom XIL (pos.2)*	*this study, derived from LJY183*
LJY191	*S288C*	*MATa trpΔ63, hisΔ200, ura3Δ::KanMX6, sir3Δ::HYG, TEL-XIL::URA3*	*URA3 at position 2399 of Chrom XIL (pos.3)*	*this study, derived from LJY184*
LJY192	*S288C*	*MATa trpΔ63, hisΔ200, ura3Δ::KanMX6, sir3Δ::HYG, TEL-XIL::URA3*	*URA3 at position 1623 of Chrom XIL (pos.4)*	*this study, derived from LJY185*
LJY193	*S288C*	*MATa trpΔ63, hisΔ200, ura3Δ::KanMX6, sir3Δ::HYG, TEL-XIL::URA3*	*URA3 at position 1373 of Chrom XIL (pos.5)*	*this study, derived from LJY186*
LJY194	*S288C*	*MATa trpΔ63, hisΔ200, ura3Δ::KanMX6, sir3Δ::HYG, TEL-XIL::URA3*	*URA3 at position 1123 of Chrom XIL (pos.6)*	*this study, derived from LJY187*
LJY195	*S288C*	*MATa trpΔ63, hisΔ200, ura3Δ::KanMX6, sir3Δ::HYG, TEL-XIL::URA3*	*URA3 at position 873 of Chrom XIL (pos.7)*	*this study, derived from LJY188*

Figure S9. List of strains used in this study. Genotype and relevant mutations are indicated for all control and ancestral strains used for evolution experiments. *Ref 37.* Mortimer, R. K. & Johnston, J. R. *Genealogy of principal strains of the yeast genetic stock center.* **Genetics 113**, 35–43 (1986).